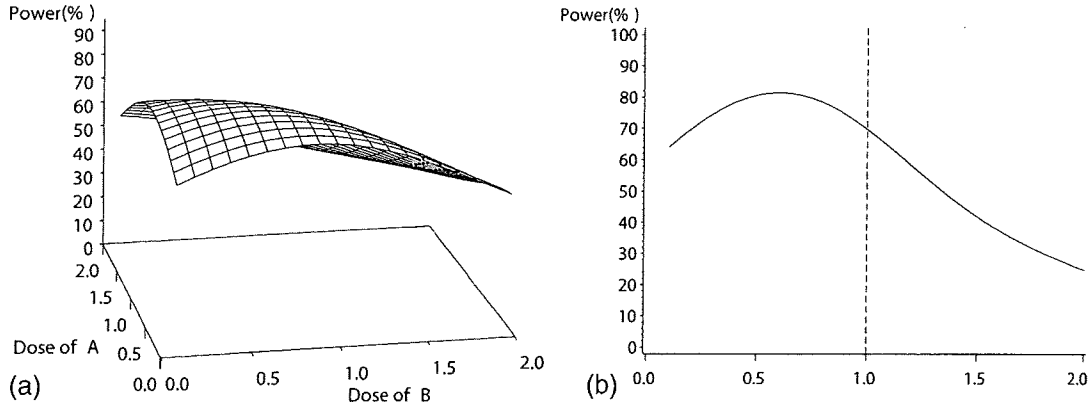

Figure 1. Power surface on the (a) dose plane and power function on the (b) dose for a simultaneous administration group with a constant surplus case (Case 1)

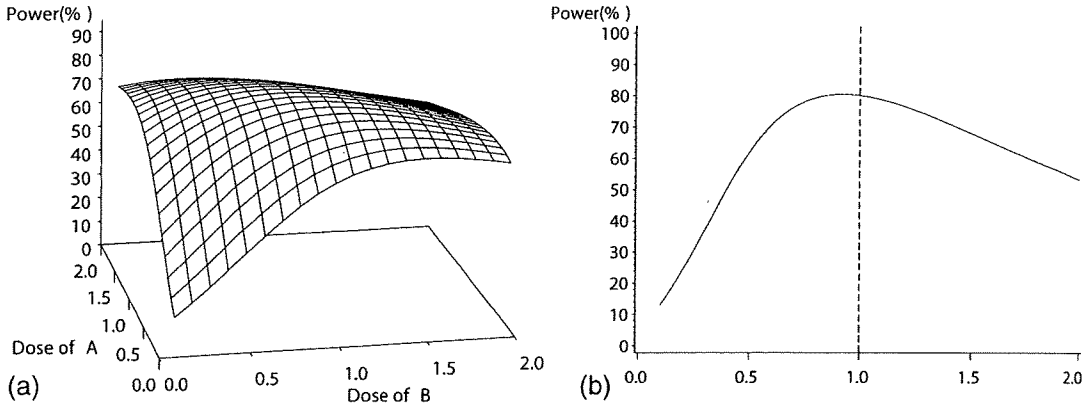

Figure 2. Power surface on the (a) dose plane and power function on the (b) dose for a simultaneous administration group with a square root surplus case (Case 2)

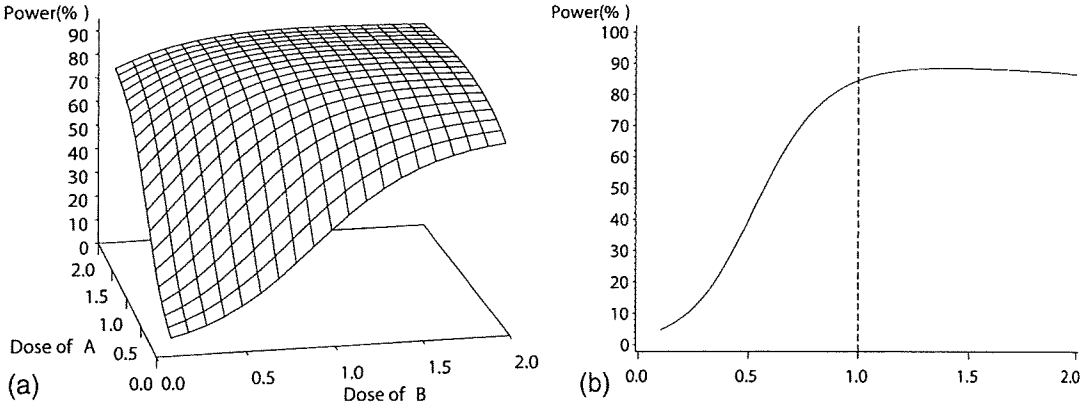

Figure 3. Power surface on the (a) dose plane and power function on the (b) dose for a simultaneous administration group with a linear surplus case (Case 3)

DOI: 10.1002/env

According to Figure 1, the power is high when the group point of the simultaneous administration group is within the triangular region and the power is low when it is located outside that region. Consequently, the design to evaluate synergism should have the group point within the triangle region. Figure 2 shows the power reaches a peak near the boundary of the triangular region and decreases apart from the triangular region as the dose increases. In consequence, the group point should be located on the boundary of triangle region. Finally, according to Figure 3, the power achieves the steady state on the boundary of the triangular region and reaches a peak slightly outside the triangular region when Δ becomes larger linearly as the dose increases. In numerical example, recommended group point in Cases 1–3 is, respectively, $(d_A, d_B) = (0.6, 0.6)$, $(0.9, 0.9)$, $(1.4, 1.4)$ and the power is 81.4%, 80.4%, 88.4%, respectively.

The sensitivity analysis was conducted to investigate the usefulness of location of the group point in the real study, such as two group points $(d_A, d_B) = (0.5, 0.5)$ and $(1.0, 1.0)$. In this section, only group points for simultaneous administration were changed in the following way and all other conditions were the same.

4.2.3. Group points for simultaneous administration.

(1) $(d_A, d_B) = (0.6, 0.6)$ (recommended in Case 1)
(2) $(d_A, d_B) = (0.9, 0.9)$ (recommended in Case 2)
(3) $(d_A, d_B) = (1.4, 1.4)$ (recommended in Case 3)
(4) $(d_A, d_B) = (1.0, 1.0)$ (on the boundary)
(5) $(d_A, d_B) = (0.5, 0.5), (1.0, 1.0)$ (real study)

Here, the total sample size for simultaneous administration groups is fixed in all group points (1)–(5). Then n_m for two groups' simultaneous design such as (5) is half of that for one group's design.

The numerical calculation was conducted under the above conditions. Table 2 summarizes the reduction of power from a recommended group point. When the group point is located close to the boundary of the triangular region, the reductions of power from a recommended group point are small. Furthermore, in the situation of real studies, the loss of power is negligible compared to that in a recommended group point. It is considered that the configuration of the group points in real study is reasonable from the statistical viewpoint.

4.3. Recommended group size

In this section, under conditions in which the total number of animals is fixed and the effect sizes are varied, we investigate the group size of the simultaneous administration group that maximizes the power.

Table 2. Reduction of power from a recommended group point in three cases

Group point (d_A, d_B)	Case 1 (constant case)	Case 2 (square root case)	Case 3 (linear case)
(0.6, 0.6)	0.0	−10.2	−34.7
(0.9, 0,9)	−7.3	0.0	−9.3
(1.4, 1.4)	−34.6	−9.7	0.0
(1.0, 1.0)	−12.2	−0.4	−5.1
(0.5, 0.5), (1.0, 1.0)	−2.0	−2.6	−19.7

n_m for two group points is half of that for one group.

DOI: 10.1002/env

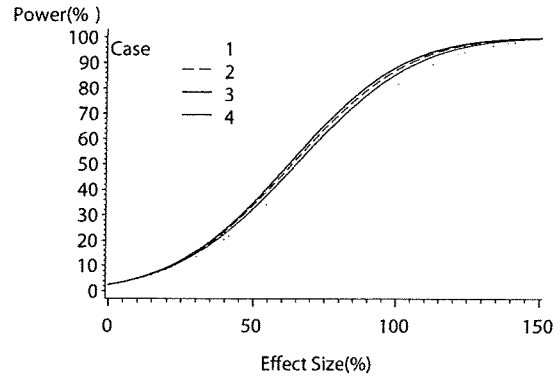

Figure 4. Relation between power and group size in four cases

4.3.1. Fixed conditions.

1. Group points for single administration: $(d_A, d_B) = (0, 0), (1, 0), (2, 0), (0, 1), (0, 2)$.
2. Group point for simultaneous administration: $(d_A, d_B) = (0.6, 0.6)$.
3. Parameters in the dose–response curve: $\beta_0 = 1.0$, $\beta_A = 1.0$, $\beta_B = 1.0$.
4. Variance σ^2: $\sigma_s^2 = \sigma_m^2 = 1.0$.
5. Nominal significance level of t-test: one-sided 2.5%.
6. Total number of animals: $n = 42$.

4.3.2. Varied conditions.

7. Group size:
   Case 1: $n_s = 6, n_m = 12$
   Case 2: $n_s = 5, n_m = 17$
   Case 3: $n_s = 4, n_m = 22$
   Case 4: $n_s = 3, n_m = 27$
8. Effect Size: $\Delta/\sigma_m = 0.1(0.1)1.5$.

Figure 4 shows the results of the numerical calculations, with the power on the vertical axis and the effect size on the horizontal axis. According to Figure 4, regardless of the effect size, Case 3 gives the maximum power. Because the group size is constrained to be an integer, it is not possible to give the most appropriate group size as a continuous value. The power becomes larger when the group size of the simultaneous administration group is set larger than that of the single administration group. When $n = 42$, what is prominent is the fact that the group size of 22 in the simultaneous administration group is nearly equal to the total number of animals in the single administration group, $4 \times 5 = 20$.

5. DISCUSSION

5.1. Conclusion under assumed conditions

In the previous section, we investigated applicable designs assuming that the response variables follow a homoscedastic normal distribution, that the dose–response relationship for single administration is

DOI: 10.1002/env

linear, that synergism is defined as a larger response obtained with simultaneous administration as compared to the dose plane obtained with single administration by assuming additivity, that there are five groups for single administration and one group for simultaneous administration, etc.

As the results of numerical calculation for the group point, when the departure Δ from additivity is proportional to square root of the dose, it is revealed that the group point for the simultaneous administration group should be on the boundary of the triangle region. Here, the results seemed to be reasonable. Because it is natural to expect that the departure Δ does not continue to increase along with the dose constantly. So, we applied these two situations as the sensitivity analysis. When the departure Δ become larger linearly along with the dose, the group point should be located slightly outside the triangle region. On the other hand, the group point should be set inside the triangle region when the departure Δ is constant. However, the group point should be placed on the boundary of the triangular region, because the reduction of power from a recommended group point is small. This means that the conventional design in the real study is appropriate.

Subsequently, with respect to the group size, we revealed that the total number of animals allocated to the simultaneous administration group should be same size as that in the single administration group.

5.2. Heteroscedasticity

When heteroscedasticity in data is expected from the past research, it is required to adjust the degree of freedom by using the Welch test. For the cases discussed in this paper, we used the Welch test, which is robust for heteroscedasticity because there is a tendency in real data for the variance to increase with an increase in responses although the number of animals is small. However, the Welch test does not control a type 1 error below the nominal significance level under heteroscedasticity. It is, therefore, required to confirm, *ex post facto*, the type 1 error when the degree of heteroscedasticity is large.

5.3. Linearity

For the cases discussed in this paper, based on advanced information, it was possible to select the dose so that there is linearity with the single administration group. This was easier due to the fact that the number of dose levels in the single administration group was small (three levels). From the experimental results, it was also confirmed that the linearity assumptions were established to some extent. When using the results in this paper, it is important to confirm the dose–response relationship in preliminary experiments or in past experiments using analogous substances. It is necessary to examine, *ex post facto*, the linearity by displaying in figure or by linearity tests.

5.4. Group size

The group size must be an integer of at least 1. In addition, the total number of animals must be a comparatively small. Under these conditions, as in this paper, it is necessary to obtain the appropriate design using numerical calculations, separately considering a combination of possible group sizes. However, in order to generalize these results, it is useful to perform power calculations, taking the group size as a continuous value. When calculating the recommended ratio of the total number of animals in the single administration group to the group size of the simultaneous administration group, the results shown in Figure 5 are obtained.

When determining the appropriate group point of the simultaneous administration group, with the departure Δ from the additivity being constant, the highest power is obtained by setting the number of

DOI: 10.1002/env

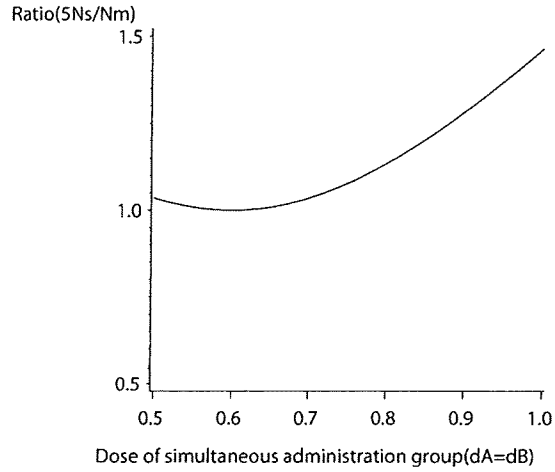

Figure 5. Recommended ratio of the group size between single administration group and simultaneous administration group

animals at a ratio of 1:1 between the single administration group and the simultaneous administration group.

When determining the simultaneous administration group on the boundary of the triangular region, a theoretical calculation shows that the allocation at a ratio of 1.464:1 is appropriate. In other words, it is best to set the total number of animals in the single administration group to be approximately 1.5 times the total number of animals in the simultaneous administration group. The reason is that because it is theoretically favorable for the accuracy of estimates based on additivity to be equal to that based on simultaneous administration.

5.5. Practical consideration on the recommended design

In the numerical examples of the previous section, we showed that the group point for the simultaneous administration on the boundary of the triangular region is not necessarily best and the recommended number of animals for the simultaneous administration group is considerably greater than those for single administration groups.

Although these results speciously imply that the design exemplified in the Subsection 4.1 should be replaced with the recommended design shown in this paper in future, we think it is not always true, because we have to take practical conditions into consideration, which were not incorporated in the assumptions to derive the recommended design.

One of them is the robustness or stability of the result of data analysis in such experiments. The situation is quite similar to that for the recommended design at linear regression analysis, for example, related to a single chemical experiment. Actually, if we can entirely assume the linearity of the dose–response relationship in regression analysis, the recommended design is to allocate a half of animals to the maximum dose and the remaining half to the minimum dose, while such design is really not adopted and animals are evenly allocated to uniformly distributed three or four doses probably to secure the robustness of the result of data analysis. Likewise, when the functional relationship of the Δ is not particularly clear, or when there is concern for the instability in squeezing the simultaneous administration group into one group in our experiments, the design with two or three simultaneous

DOI: 10.1002/env

administration groups within the triangular region must be practical. Since the mathematical formulation in such condition could not be established up to present due to its difficult nature, we left it for future investigation.

5.6. *Other issues for future investigation*

When the number of test substances is 3 or more, there needs to be strict controls for the number of required animals. Therefore, a design must be determined by examining the design conditions in detail for each case. Under this condition, an investigation following the same approach as in this paper is necessary. This is another problem to be addressed in future research.

In this paper, we introduced a test statistic by using the unweighted least squares method. The weighted least squares method must be considered when the rules for the size of variance are understood from past research, such that variance linearly becomes larger along with the dose. The specific design in this instance is also to be investigated in the future.

ACKNOWLEDGMENT

We thank Professor Takashi Sozu at Osaka University for his assistance in the preparation of this paper. We are grateful to the Editor-in-Chief and two anonymous reviewers for their comments that greatly improved this paper.

REFERENCES

Abdelbasit KM, Plackett RL. 1982. Experimental design for joint action. *Biometrics* **38**: 171–179.
Berenbaum MC. 1989. What is synergy? *Pharmacological Review* **41**: 93–141.
Gennings C, Schwartz P, Carter WH, Simmons JE. 1997. Detection of departures from additivity in mixtures of many chemicals with a threshold model. *Journal of Agricultural, Biological, and Environmental Statistics* **2**: 198–211.
Gennings C, Carter WH. 1995. Utilizing concentration-response data from individual components to detect statistically significant departures from additivity in chemical mixture. *Biometrics* **51**: 1264–1277.
Hasegawa R, Yoshimura I, Imaida K, Ito N, Shirai T. 1996. Analysis of synergism in hepatocarcinogenesis based on preneoplastic foci induction by 10 heterocyclic amines in the rat. *Japanese Journal of Cancer Research* **87**: 1125–1133.
Hewlett PS, Plackett RL. 1959. A unified theory for quantal response to mixtures of drugs: noninteractive action. *Biometrics* **15**: 591–610.
Kanno J, Onyon L, Haseman J, Fenner-Crisp P, Axhby J, Owens W. 2001. The OECD program to validate the rat uterotrophic bioassay to screen compounds for *in vivo* estrogenic response: phase 1. *Environmental Health Perspectives* **109**: 785–794.
Kelly C, Rice J. 1990. Monotone smoothing with application to dose-response curve and the assessment of synergism. *Biometrics* **46**: 1071–1085.
Laska EM, Meisner MJ. 1989. Testing whether an identified treatment is best. *Biometrics* **45**: 1139–1151.
Matsunaga N, Kanno J, Yoshimura I. 2003. A statistical method for judging synergism application to an endocrine disruptor animal experiment. *Environmetrics* **14**: 213–222.
Machado SG, Robinson GA. 1994. A direct, general approach based on isobologram for assessing the joint action of drugs in pre-clinical experiment. *Statistics in Medicine* **13**: 2289–2309.
Roy P, Esteve J. 1998. Using relative risk models for estimating synergy between two risk factors. *Statistics in Medicine* **17**: 1357–1373.
Straetemans R, O'Brien T, Wouters L, Dun JV, Janicot M, Bijnens L, Burzykowski T, Aerts M. 2005. Design and analysis of drug combination experiments. *Biometrical Journal* **47**: 299–308.
Tan M, Fang HB, Tian GL, Houghton PJ. 2003. Experimental design and sample size determination for testing synergism in drug combination studies based on uniform measures. *Statistics in Medicine* **22**: 2091–2100.

Cellular distributions of molecules with altered expression specific to thyroid proliferative lesions developing in a rat thyroid carcinogenesis model

Gye-Hyeong Woo,[1] Miwa Takahashi,[1] Kaoru Inoue,[1] Hitoshi Fujimoto,[1] Katsuhide Igarashi,[2] Jun Kanno,[2] Masao Hirose,[1,3] Akiyoshi Nishikawa[1] and Makoto Shibutani[1,4,5]

Divisions of [1]Pathology, [2]Molecular Toxicology, National Institute of Health Sciences, Setagaya-ku, Tokyo; [3]Food Safety Commission, Chiyoda-ku, Tokyo; [4]Laboratory of Veterinary Pathology, Tokyo University of Agriculture and Technology, Fuchu-shi, Tokyo, Japan

(Received November 15, 2008/Revised December 25, 2008/Accepted December 26, 2008/Online publication February 26, 2009)

To identify differentially regulated molecules related to early and late stages of tumor promotion in a rat two-stage thyroid carcinogenesis model by an antithyroid agent, sulfadimethoxine, microarray-based microdissected lesion-specific gene expression profiling was carried out. Proliferative lesions for profiling were divided into two categories: (i) focal follicular cell hyperplasias (FFCH) and adenomas (Ad) as early lesions; and (ii) carcinomas (Ca) as more advanced. In both cases, gene expression was compared with that in surrounding non-tumor follicular cells. Characteristically, upregulation of cell cycle-related genes in FFCH + Ad, downregulation of genes related to tumor suppression and transcription inhibitors of inhibitor of DNA binding (Id) family proteins in Ca, and upregulation of genes related to cell proliferation and tumor progression in common in FFCH + Ad and Ca, were detected. The immunohistochemical distributions of molecules included in the altered expression profiles were further examined. In parallel with microarray data, increased localization of ceruloplasmin, cyclin B1, and cell division cycle 2 homolog A, and decreased localization of poliovirus receptor-related 3 and Id3 were observed in all types of lesion. Although inconsistent with the microarray data, thyroglobulin immunoreactivity appeared to reduce in Ca. The results thus suggest cell cycling facilitation by induction of M-phase-promoting factor consisting of cyclin B1 and cell division cycle 2 homolog A and generation of oxidative responses as evidenced by ceruloplasmin accumulation from an early stage, as well as suppression of cell adhesion involving poliovirus receptor-related 3 and inhibition of cellular differentiation regulated by Id3. Decrease of thyroglobulin in Ca may reflect dedifferentiation with progression. (*Cancer Sci* 2009; 100: 617–625)

Although clinically recognized thyroid Ca constitute less than 1% of all human malignant tumors, it is the most common endocrine cancer (90% of cases) and is responsible for more deaths than all other endocrine cancers combined.[1] Ca of the thyroid is usually of follicular cell origin, but the medullary carcinoma arises from parafollicular or C cells. In humans, causative factors for thyroid Ca are not well understood except for secondary occurrence after radiotherapy.[2] In rats, on the other hand, thyroid follicular cell tumors can be produced by administration of antithyroid agents, such as by propylthiouracil,[3] methimazole,[4] and 3-amino-1,2,4-triazole,[5] in an initiation-promotion model.

Many chemicals that can induce thyroid tumors in rodents cause disruption of the thyroid–pituitary axis through induction of hypothyroidism.[6] The putative mechanism for this carcinogenesis is believed to be non-genotoxic, decrease in the serum levels of triiodothyronine and thyroxine causing suppression of negative feedback through the pituitary and an increase in serum TSH. TSH then stimulates thyroid functions, including growth and proliferation of follicular cells.[7,8] However, detailed molecular mechanisms remain to be resolved.[6]

SDM is a broad-spectrum antimicrobial sulfonamide that has been shown to effectively induce thyroid follicular cell tumors in a rat two-stage thyroid carcinogenesis model after initiation with DHPN.[9] The anti-thyroidal effects of this drug are mediated through inhibition of iodination reactions catalyzed by thyroid peroxidase, resulting in reduction of thyroid hormone synthesis and increased levels of TSH in the bloodstream.[10]

Histological lesion-specific gene expression profiling provides valuable information on the mechanisms underlying lesion development. We have established molecular analysis methods for DNA, RNA, and proteins in paraffin-embedded small-tissue specimens utilizing an organic solvent-based fixative, methacarn,[11–13] and applied them for analyses of microdissected lesions.[14,15] With regard to mRNA expression analysis, expression fidelity in the methacarn-fixed paraffin-embedded tissues was found to be very close to that in the unfixed frozen tissues in both the real-time RT-PCR and oligonucleotide microarray systems, suggesting a great advantage of methacarn in analyses of microdissected lesions after paraffin embedding.[14,15]

In the present study, to identify differentially regulated molecules related to thyroid carcinogenesis through hypothyroidism, we carried out global gene expression profiling of early and late-stage proliferative lesions obtained after promotion with SDM in a rat two-stage carcinogenesis model. Localization of representative molecules showing altered expression was further analyzed immunohistochemically.

Materials and Methods

Chemicals and animals. DHPN (CAS no. 53609-64-6) and SDM (CAS no. 122-11-2) were purchased from Nacalai Tesque (Kyoto, Japan) and Sigma (St Louis, MO, USA), respectively. Male 5-week-old F344 rats were purchased from Japan SLC (Hamamatsu, Japan) and housed four to five rats per polycarbonate cage with sterilized softwood chips as bedding in a barrier-sustained animal room conditioned at 24 ± 1°C and 55 ± 5% humidity, with a 12:12 h L : D cycle. They received CRF-1 (Oriental Yeast Co., Tokyo, Japan) as a basal diet and water *ad libitum* throughout the experimental period, including the 1 week of acclimation.

Experimental design. At 6 weeks of age, 30 rats were injected subcutaneously with 2800 mg/kg body weight DHPN. Another

[5]To whom correspondence should be addressed. E-mail: mshibuta@cc.tuat.ac.jp

Abbreviations: Ad, adenoma; Ca, carcinoma; Ccnb1, cyclin B1; Cdc2, cell division cycle 2; DHPN, *N*-bis(2-hydroxypropyl)nitrosamine; FFCH, focal follicular cell hyperplasia; Id, inhibitor of DNA binding; IGSF, immunoglobulin superfamily; NTF, non-tumor follicles; PCR, polymerase chain reaction; Pvrl3, poliovirus receptor-related 3; RT, reverse transcription; SDM, sulfadimethoxine; TSH, thyroid-stimulating hormone.

doi: 10.1111/j.1349-7006.2009.01094.x

group of nine animals was injected with the vehicle saline as non-treated controls. One week later, 25 DHPN-initiated animals were administered SDM at 1000 p.p.m. in the drinking water *ad libitum* for up to 15 weeks. The other five DHPN-initiated animals were maintained on tap water for 10 weeks as a DHPN-alone group. At week 10 after SDM treatment, 10 animals were killed for microdissection of FFCH + Ad as well as NTF in each animal. The other SDM-promoted animals were further maintained until week 15, when 12 rats were killed for microdissection of Ca. Five untreated controls and the DHPN-alone group were killed at week 10 of SDM promotion, and the four remaining untreated controls at week 15. All animals were killed by exsanguination from the abdominal aorta under deep anesthesia with ether. The animal protocol was reviewed and approved by the Animal Care and Use Committee of the National Institute of Health Sciences, Japan.

Preparation of tissue specimens and microdissection. Caudal halves of the bilateral thyroid tissues of SDM-promoted animals were immersed in methacarn solution for 2 h at 4°C.[11] Tissue samples were then dehydrated, immersed in xylene, and embedded in paraffin as described previously.[15] Embedded tissue blocks were stored at 4°C until microdissection.[16]

For microarray analysis, 4 μm-thick sections between 10 16 μm-thick serial sections were prepared. The 16 μm-thick sections were mounted onto PEN-foil film (Leica Microsystems, Welzlar, Germany) overlaid on glass slides, dried in an incubator overnight at 37°C, and then stained using an LCM staining kit (Ambion, Austin, TX, USA). All microdissections were carried out within 2 h of tissue staining. The histopathological identity of each FFCH, Ad, and Ca, as well as NTF, was determined under microscopic observation of the adjacent 4 μm-thick sections stained with hematoxylin–eosin according to published criteria (Fig. 1).[17] In the present carcinogenesis model with SDM promotion, capsular invasive carcinomas are generated in addition to less-frequent parenchymal Ca.[18] In the present study, parenchymal proliferative lesions including the latter were subjected to laser microbeam microdissection (Leica Microsystems). Approximately 20 sections of bilateral thyroids were subjected to microdissection in one animal, and the microdissected samples (NTF, FFCH + Ad, and Ca) were collected and stored in separate 1.5-mL sample tubes at −80°C until extraction of total RNA.

RNA isolation, amplification, and microarray analysis. Total RNA extraction from each histological sample and quantitation of the RNA yield were carried out according to methods described previously.[15]

For microarray analysis, equal amounts of extracted total RNA samples from two animals were mixed (100 ng/sample) and subjected to amplification, consisting of RT and subsequent two-step *in vitro* transcription, using a MessageAmp II aRNA Kit (Ambion).

Second-round-amplified biotin-labeled antisense RNA was subjected to hybidization with a GeneChip Rat Genome 230 2.0 Array (Affymetrix Inc., Santa Clara, CA, USA). RNA samples collected from two animals were subjected to analysis with individual microarrays (n = 5/histological preparation).

Selection of genes and normalization of expression data were carried out using GeneSpring software (ver7.2; Silicon Genetics, Redwood City, CA, USA). To normalize chip-wide variation in intensity, per chip normalization was performed by dividing the signal strength for each gene with the level of the 50th percentile of the measurement in the chip, and dividing the value by the average intensity in the samples of NTF. Genes showing signals judged to be 'absent' in all 10 samples of NTF and each proliferative lesion group (FFCH + Ad or Ca) for comparison were excluded. Then, genes showing expression change with differences at least 2-fold in magnitude in the proliferative lesion groups from the NTF, as well as the 'presence' signal in more than four of five samples in the histological lesion group (NTF or each proliferative lesion group) showing higher expression values in comparison, were selected. Genes showing altered expression in common in both FFCH + Ad and Ca were also selected.

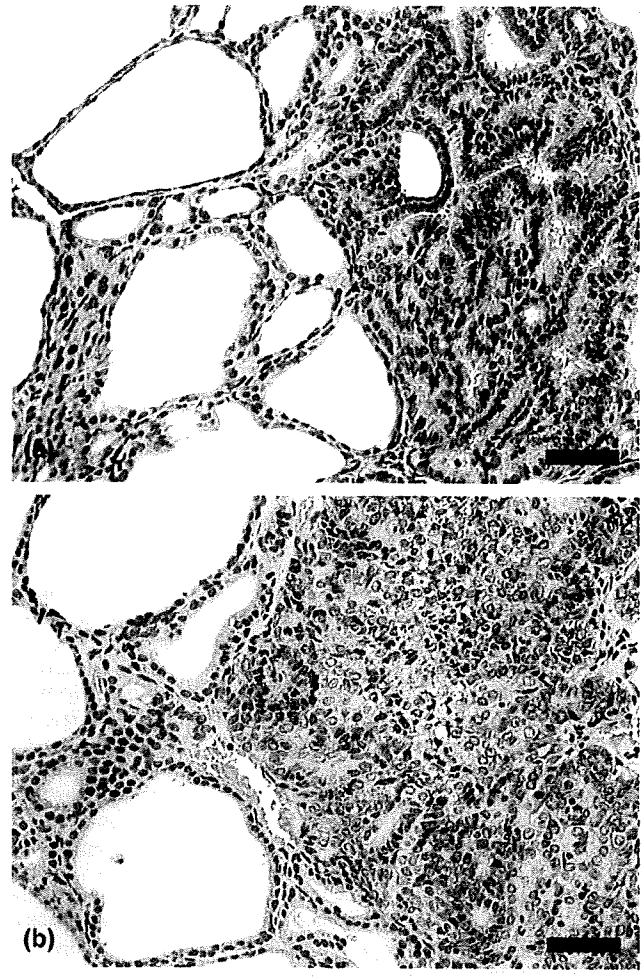

Fig. 1. Representative proliferative lesions developing after promotion with sulfadimethoxine (SDM) for (a) 10 or (b) 15 weeks in a rat two-stage thyroid carcinogenesis model. (a) Adenoma with follicular features, showing expansive growth with minor atypia. (b) Carcinoma showing obvious cellular atypia, consisting of follicular and solid growth elements with structural irregularity. Note focal necrosis and fibrosis. Hematoxylin–eosin staining. Scale bars = 50 μm.

Real-time RT-PCR. Quantitative real-time RT-PCR was carried out for confirmation of expression values obtained with microarrays using an ABI Prism 7900HT (Applied Biosystems, Foster City, CA, USA). The following 11 genes (eight upregulated and three downregulated in proliferative lesions) were selected as targets: chitinase 3-like 1, ceruloplasmin, solute carrier family 2 (facilitated glucose transporter) member 3, solute carrier family 16 (monocarboxylic acid transporters) member 6, glucagon, prolactin receptor, phosphatidylinositol 4-kinase type 2α, and actinin α1 as upregulated examples; and *Pvrl3*, retinoic acid induced 3, and glucosaminyl (*N*-acetyl) transferase 1 core 2 as downregulated examples. RT was carried out using first-round antisense RNA prepared for microarray analysis. Real-time PCR analysis of ceruloplasmin, glucagon, and glucosaminyl (*N*-acetyl) transferase 1 core 2 was carried out using ABI Assays-on-Demand TaqMan probe and primer sets from Applied Biosystems (available at https://products.appliedbiosystems.com/ab/en/US/

doi: 10.1111/j.1349-7006.2009.01094.x

Table 1. Sequences of primers used for real-time reverse transcription–polymerase chain reaction with the SYBR Green detection system

Gene	Accession no.	Sense/Antisense	Sequence
Chi3l1	AA945643	Sense	5′-TCGTTAACAGGGATGACCTGTATCT-3′
		Antisense	5′-GGGTAGGACGGTGGGATTGT-3′
Slc2a3	AA901341	Sense	5′-AAGCTGGCCATTGGCAAAT-3′
		Antisense	5′-CTAGCCTCTTGTGCTCCTCCAT-3′
Slc16a6	AA859652	Sense	5′-AAAGGTGTTTCGACTGCATTCTC-3′
		Antisense	5′-CCCCATGTACCAAGCACTGTT-3′
Prlr	AW142962	Sense	5′-TGTCGCATAAGGTCCCCTCTT-3′
		Antisense	5′-GCTTGGCAATTTGTAGGGAAAG-3′
Pi4KII	BE097981	Sense	5′-CCCCTTTCTCTTTCCTTCTGGTA-3′
		Antisense	5′-ACAGCAAGTTCCAGGACAGTCA-3′
Actn1	BE119221	Sense	5′-AAGAAGGCGGTGTCTGTAAGCT-3′
		Antisense	5′-CCGTCCCTTGGCTTTGAA-3′
Pvrl3	AW525315	Sense	5′-GGCAAGACACTGGTTCTACACAAT-3′
		Antisense	5′-AAGGCCCGAAGAATGTTTTTC-3′
Rai3	BI276110	Sense	5′-GGAGCAAGTGCCAGGAATTTAT-3′
		Antisense	5′-CAGTTTTTTCCAGCCAGGAGAA-3′

Actn1, actinin α1; Chi3l1, chitinase 3-like 1; Pi4KII, phosphatidylinositol 4-kinase type 2α; Prlr, prolactin receptor; Pvrl3, poliovirus receptor-related 3; Rai3, retinoic acid induced 3; Slc2a3, solute carrier family 2 (facilitated glucose transporter) member 3; Slc16a6, solute carrier family 16 (monocarboxylic acid transporters) member 6.

adirect/ab?cmd=catNavigate2&catID=601267) (n = 5/histological preparation). For measurement of transcript levels of chitinase 3-like 1, solute carrier family 2 (facilitated glucose transporter) member 3, solute carrier family 16 (monocarboxylic acid transporters) member 6, prolactin receptor, phosphatidylinositol 4-kinase type 2α, actinin α1, *Pvrl3*, and retinoic acid induced 3, primer sets were designed using Primer Express software (Version 2.0; Applied Biosystems), and the corresponding primer sequences are shown in Table 1. Amplified transcript levels were measured with the SYBR Green detection system (n = 5/histological preparation). For quantification of expression data, a standard curve method was applied using the first-round antisense RNA prepared for microarray analysis from NTF as a standard sample. Expression values were normalized to two housekeeping genes, glyceraldehyde 3-phosphate dehydrogenase and hypoxanthine-guanine phosphoribosyltransferase, as described previously.[14]

Immunohistochemistry. The cranial halves of the bilateral thyroids of SDM-promoted animals were subjected to fixation in 10% phosphate-buffered formalin (pH 7.4) solution for 2 days at room temperature, and prepared for histopathological examination. In untreated controls and DHPN-alone cases, whole thyroid tissue was fixed in buffered formalin and prepared similarly.

Immunohistochemistry was carried out with antibodies against ceruloplasmin (clone 8, mouse IgG_1, 1:50; BD Transduction Laboratories, San Jose, CA, USA), Ccnb1 (clone V152, mouse IgG_1, 1:100; Thermo Fisher Scientific Inc., Fremont, CA, USA), Cdc2 (clone A17, mouse IgG_{2a}, 1:200; GeneTex, San Antonio, TX, USA), thyroglobulin (clone SPM221, mouse IgG_1, 1:250; Spring Bioscience, Fremont, CA, USA), Pvrl3 (goat IgG, 1:100; R&D Systems, Minneapolis, MN, USA), and Id3 (rabbit IgG, 1:100; ProteinTech Group, Chicago, IL, USA). For confirmation of positive immunoreactivity of antigens examined, normal rat tissues, such as the liver for ceruloplasmin,[19] duodenal mucosa for Ccnb1 and Cdc2, and thyroid for thyroglobulin,[20] Pvrl3, and Id3, were used. For each antigen, subcellular or extracellular localization was examined and compared to the cases previously reported.[21–26] Optimal conditions for antigen retrieval were also determined using positive control tissues. For antigen retrieval, deparaffinized sections were heated in 10 mM citrate buffer (pH 6.0) by autoclaving for 10 min before incubation with the Ccnb1 and Pvrl3 antibodies, or for 20 min before incubation for ceruloplasmin, Cdc2, and Id3. No antigen retrieval treatment was carried out for thyroglobulin. Immunodetection was carried out utilizing a Vectastain Elite ABC kit (Vector Laboratories, Burlingame, CA, USA), with 3,3′-diaminobenzidine/H_2O_2 as the chromogen, as described previously.[15] As negative controls for immunoreactivity, normal serum from mouse, goat, or rabbit was applied to rat positive control tissues with appropriate dilutions instead of the primary antibodies. Sections were counterstained with hematoxylin.

Analysis of immunoreactivity. For all antigens examined in the present study, immunoreactivity was essentially unaltered in the thyroids between the groups of untreated controls and DHPN alone, and these animals did not develop any proliferative lesion. Therefore, immunoreactivity scores in these groups were counted together and represented as 'normal follicular cells' with three randomly selected microscopic areas at 200-fold magnification in one animal. Animals examined for 'normal follicular cells' were nine untreated controls and five treated with DHPN. In the SDM-promoted cases, immunoreactivity scores were counted in the histological categories of NTF, FFCH + Ad, and Ca. With regard to NTF, three randomly selected microscopic areas at 200-fold magnification were subjected to evaluation for each animal. With Ca, both capsular invasive and parenchymal Ca were analyzed. Immunoreactivity in each histological type was not essentially different between the cases after 10 and 15 weeks of promotion, and therefore immunolocalization scores were counted together for these two time points. The numbers of animals examined for proliferative lesions and surrounding NTF were 10 and 11 after 10 and 15 weeks of promotion, respectively.

For ceruloplasmin, Ccnb1, Cdc2, Id3, and thyroglobulin, immunolocalization was scored as 0 (negative), 1 (slight), 2 (moderate), or 3 (prominent). In the case of Pvrl3, scores were 0 (negative), 1 (partially positive), or 2 (positive). Detailed criteria for the immunoreactivity for each molecule given in Table 2 were determined after due consultation of two independent pathologists. Immunoreactivity score in each lesion was double-checked by one pathologist and then cross-checked by another pathologist.

Data analysis. Expression values from the real-time RT-PCR were analyzed by Student's or Welch's t-test following a test for equal variance. Scores for immunoreactivity were assessed with Mann–Whitney's U-test, comparing NTF and normal follicles, FFCH + Ad or Ca. For the microarray data, the statistical analysis was carried out with GeneSpring software, and the significance

Table 2. Scoring criteria for immunohistochemical localization

Molecule	Immunolocalization for evaluation	Score of immunoreactivity			
		0	1	2	3
Ceruloplasmin	Luminal cellular surface	—	Weakly positive, a few follicles	Strongly positive, focal follicular populations	Strongly positive, majority of follicles
Ccnb1	Cytoplasm	—	Weakly positive, a few cells	Weakly positive, majority of cells	Strongly positive, majority of cells
Cdc2	Cytoplasm and nucleus	—	1–10 cells/400× field	10–30 cells/400× field	> 30 cells/400× field
Thyroglobulin	Cytoplasm	—	< 20% cells	20–70% cells	> 70% cells
Pvrl3	Intercellular membrane	—	Focally positive	Entirely positive	Not applied
Id3	Nucleus	—	Weakly positive, a few cells	Weakly positive, majority of cells	Strongly positive, majority of cells

Ccnb1, Cyclin B1; Cdc2, cell division cycle 2; Id3, inhibitor of DNA binding 3; Pvrl3, poliovirus receptor-related 3.

of gene expression changes was analyzed by Student's *t*-test or ANOVA between NTF and normal follicles, FFCH + Ad or Ca.

Results

Microarray analysis. As genes showing altered expression specifically in FFCH + Ad, 40 examples were upregulated and 20 examples were downregulated, as compared with surrounding NTF (Table 3; Supporting Tables S1, S2). In the Ca cases, the numbers of genes specifically upregulated and downregulated were 69 and 142, respectively. Representative genes with known annotations associated with carcinogenesis are listed in Table 3. Interestingly, a cluster of cell cycle-related genes were found to be upregulated specifically in FFCH + Ad, such as ubiquitin-like with PHD and RING finger domains 1, kinesin family member 23, cyclin A2, M-phase phosphoprotein, topoisomerase (DNA) 2α, Cdc2 homolog A, Ccnb1, and cyclin-dependent kinase inhibitor 3. Extracellular matrix proteins, laminin γ2, and fibronectin 1 also showed upregulation in FFCH + Ad. No particular functional cluster was observed for downregulated genes in FFCH + Ad cases. Among the upregulated genes in Ca, examples with functions in transport (ceruloplasmin) and biosynthesis (thyroglobulin) were found, whereas downregulated genes typically involved functions in tumor suppression, such as: decorin, reversion-inducing-cysteine-rich protein with kazal motifs, creatine kinase mitochondrial 1 ubiquitous, retinoblastoma 1, lysyl oxidase, and NAD(P)H dehydrogenase quinine 1. Transcript levels for genes encoding signal transduction molecules and transcription factors were also downregulated in Ca. All isoforms of Id were found to be reduced.

With regard to genes showing altered expression in common in FFCH + Ad and Ca, totals of 93 and 53 were upregulated and downregulated, respectively (Table 4; Supporting Table S3). Upregulated genes included examples linked to transport, cell proliferation, and tumor progression. In particular, multiple gene probes in the array showed increased signals for ceruloplasmin and solute carrier family 16 (monocarboxylic acid transporters) member 6. Among the genes that showed downregulation, no particular functional clusters were apparent. Two gene probes for *Pvrl3* in the array demonstrated downregulation. Real-time RT-PCR for validation of microarray data was carried out for 11 genes showing commonly altered expression with FFCH + Ad and Ca, eight upregulated and three downregulated, the results being summarized in Table 5. In both FFCH + Ad and Ca, many expression changes were similar with the two analysis systems, despite a lower magnitude of alteration observed with PCR data for the upregulated genes when the values were normalized to hypoxanthine-guanine phosphoribosyltransferase levels. With regard to downregulated genes, variability of PCR data in the NTF after normalization to the hypoxanthine-guanine phosphoribosyltransferase level was slightly higher than with glyceraldehyde 3-phosphate dehydrogenase (data not shown), and therefore statistical significance was not attained for FFCH + Ad.

Immunolocalization in the thyroid in relation to proliferative lesions. Ceruloplasmin was immunolocalized mainly at the luminal surfaces of cell membranes of follicular cells, almost specific to the proliferative lesions (Fig. 2a). Diffuse or granular immunoreactivity was also observed in the follicular lumina of lesions showing cell surface immunoreactivity. In parallel with the upregulation of transcript levels both in microarray and real-time RT-PCR analyses, immunolocalization of ceruloplasmin was specifically observed in all types of proliferative lesions, with statistical significance in the scores as compared with NTF. Although the intensity was weak, increased cytoplasmic staining was also observed in some Ca.

Ccnb1 was immunolocalized in the cytoplasm of follicular cells with fine granular immunoreactivity (Fig. 2b). In the normal follicles and NTF, weak and sparse immunolocalization was typical. In the proliferative lesions, the expression pattern of this molecule was either sparse or diffuse, and staining was weak with the former and either weak or strong with the latter. In parallel with upregulation of transcript levels in microarray analysis, a significant increase in the immunolocalization scores was observed in FFCH + Ad as compared with surrounding NTF. Although statistically significant elevation was still evident, immunoreactivity was less intense in Ca than in FFCH + Ad.

Immunoreactivity of Cdc2 was strong and localized both to the cytoplasm and nucleus of tumor follicular cells (Fig. 2c). In the normal follicles and NTF, immunoreactive cells were rather few. Although microarray data showed upregulation only in FFCH + Ad, both FFCH + Ad and Ca showed statistically significant increases in the immunolocalization scores as compared with NTF. Ca demonstrated the highest scores.

Thyroglobulin showed strong and granular immunolocalization in the cytoplasm of normal and non-tumor follicular cells as well as diffuse immunoreactivity in the follicular lumina (Fig. 2d). Although microarray data showed upregulation of the transcript levels in Ca, follicular proliferative lesions showed large variability in the immunoreactivity, and Ca showed a significant decrease in immunolocalization scores as compared with NTF.

Pvrl3 showed intercellular membrane immunolocalization in the normal and non-tumor follicular cells (Fig. 2e). With both FFCH + Ad and Ca, in parallel with the downregulation of the transcript levels common to microarray and real-time RT-PCR analyses, statistically significant decreased immunolocalization scores were observed as compared with NTF. However, the magnitude of the decrease in FFCH + Ad was stronger than in the Ca case, contrasting with the transcript data.

Inhibitor of DNA binding 3 showed nuclear immunoexpression in normal and non-tumor follicular cells (Fig. 2f). Although microarray analysis showed statistically significant downregulation of transcript levels only in Ca, statistically significant decreases

doi: 10.1111/j.1349-7006.2009.01094.x

Table 3. List of representative genes with known functional annotations associated with carcinogenesis showing altered expression specifically in thyroid proliferative lesions of each category induced in rats using a two-stage thyroid carcinogenesis model (≥2-fold, ≤0.5-fold)†

Gene function	Accession no.	Gene title	Symbol	FFCH + Ad	Ca
FFCH + Ad					
Upregulated genes (of 40 genes in total)					
Cell cycle	BE098732	Ubiquitin-like, containing PHD and RING finger domains, 1	Uhrf1	2.43	1.81
Cell cycle	BE113443	Kinesin family member 23‡	Kif23	2.20	1.09
Cell cycle	AA998516	Cyclin A2	Ccna2	2.13	1.29
Cell cycle	BM385445	Topoisomerase (DNA) 2α	Top2a	2.12	1.37
Cell cycle	BE110723	M-phase phosphoprotein 1‡	Mphosph1	2.09	1.35
Cell cycle	NM_019296	Cell division cycle 2 homolog A (*S. pombe*)	Cdc2a	2.04	1.45
Cell cycle	X64589	Cyclin B1	Ccnb1	2.01	1.40
Cell cycle	BE113362	Cyclin-dependent kinase inhibitor 3‡	Cdkn3	1.97	1.18
Metastasis	BM385282	Laminin, γ2	Lamc2	2.90	1.25
Metastasis	AA893484	Fibronectin 1	Fn1	2.16	1.40
Downregulated genes (of 20 genes in total)					
Metastasis	BE117767	Immunoglobulin superfamily, member 4A‡	Igsf4a	0.46	0.73
Cell differentiation	BG666709	N-myc downstream regulated 4	Ndr4	0.50	0.51
Ca					
Upregulated genes (of 69 genes in total)					
Biosynthesis	AI500952	Thyroglobulin	Tg	1.72	2.65
Transport	AF202115	Ceruloplasmin	Cp	1.99	2.45
Transport	BE106526	Solute carrier family 6 (neurotransmitter transporter, GABA), member 11	Slc6a11	1.44	1.98
Cell growth	M57668	Prolactin receptor	Prlr	1.78	2.42
Cell cycle	NM_133578	Dual specificity phosphatase 5	Dusp5	1.74	2.02
Proto-oncogene	NM_012874	v-ros UR2 sarcoma virus oncogene homolog 1 (avian)	Ros1	1.59	1.98
Metastatic regulator	AI175048	Sine oculis homeobox homolog 1 (*Drosophila*)	Six1	1.62	1.96
Glycolysis	BI294137	Hexokinase 2	Hk2	1.20	1.87
Downregulated genes (of 142 genes in total)					
Tumor suppressor	BM390253	Decorin	Dcn	0.76	0.27
Tumor suppressor	AW523759	Reversion-inducing-cysteine-rich protein with kazal motifs‡	Reck	0.65	0.32
Tumor suppressor	BI301453	Creatine kinase, mitochondrial 1, ubiquitous	Ckmt1	0.49	0.35
Tumor suppressor	AI178012	Retinoblastoma 1	Rb1	0.75	0.38
Tumor suppressor	NM_017061 (BI304009)	Lysyl oxidase	Lox	0.81 (0.91)	0.39 (0.49)
Tumor suppressor	J02679	NAD(P)H dehydrogenase, quinone 1	Nqo1	0.57	0.42
Signal transduction	U78517	cAMP-regulated guanine nucleotide exchange factor II	Rapgef4	0.65	0.32
Signal transduction	AA945708	Calcitonin receptor-like	Calcrl	0.59	0.34
Signal transduction	BI295477	G protein-coupled receptor 116	Gpr116	0.61	0.45
Signal transduction	NM_030829	G protein-coupled receptor kinase 5	Gprk5	0.66	0.48
Cell adhesion	NM_031050	Lumican	Lum	0.99	0.33
Transcription	AF000942	Inhibitor of DNA binding 3, dominant negative helix-loop-helix protein	Id3	0.57	0.33
Transcription	BE116009	Inhibitor of DNA binding 4	Idb4	0.56	0.40
Transcription	NM_053713	Kruppel-like factor 4 (gut)	Klf4	0.67	0.40
Transcription	M86708	Inhibitor of DNA binding 1, helix-loop-helix protein (splice variation)	Id1	0.64	0.44
Transcription	AI008792	Inhibitor of DNA binding 2, dominant negative helix-loop-helix protein	Id2	0.68	0.48
Metastasis suppressor	AI578087 (AW435343)	transmembrane 4 superfamily member 1‡	Tm4sf1	0.64 (0.74)	0.36 (0.48)
Apoptosis	AA892770	Glutamate-cysteine ligase, catalytic subunit	Gclc	0.61	0.41
Tumor metastasis	NM_133526	Transmembrane 4 superfamily member 3	Tm4sf3	0.70	0.41

Ad, adenoma; Ca, carcinoma; FFCH, focal follicular cell hyperplasias.
†Proliferative lesions were divided into two categories, i.e. FFCH + Ad and Ca.
‡Predicted gene identity.

in the nuclear immunolocalization scores were also observed in FFCH + Ad.

Discussion

With the present microdissected lesion-specific gene expression profiling, alteration was found for 60 genes specifically in FFCH + Ad, 211 genes specifically in Ca, and 146 genes in common in both, as compared with surrounding NTF. On selection of these with known annotations associated with carcinogenesis, we found upregulation of cell cycle-related genes specifically in the early proliferative lesions, represented by FFCH and Ad. In the advanced Ca lesions, downregulation of genes related to tumor suppression and those encoding

Table 4. List of representative genes with known functional annotations associated with carcinogenesis showing altered expression in common with all types of thyroid proliferative lesions induced in rats using a two-stage thyroid carcinogenesis model (≥2-fold, ≤0.5-fold)†

Gene function	Accession no.	Gene title	Symbol	FFCH + Ad	Ca
Upregulated genes (of 93 genes in total)					
Adhesion	AA945643	Chitinase 3-like 1	Chi3l1	7.46	8.55
Adhesion	AI169104	Platelet factor 4	Pf4	2.52	3.71
Angiogenesis	NM_021751	Prominin 1	Prom1	4.26	5.53
Transport	NM_012532 (AF202115)	Ceruloplasmin	Cp	3.32 (2.43)	4.12 (2.79)
Transport	AA901341	Solute carrier family 2 (facilitated glucose transporter), member 3	Slc2a3	2.68	2.53
Transport	AA859652 (BG372184)	Solute carrier family 16 (monocarboxylic acid transporters), member 6	Slc16a6	2.28 (2.25)	2.33 (2.24)
Cell proliferation	AF411318	Metallothionein	Mt1a	2.11	3.77
Cell proliferation	AA819913	Carbohydrate (keratan sulfate Gal-6) sulfotransferase 1‡	Chst1	2.77	3.75
Cell proliferation	NM_022278	Glutaredoxin 1 (thioltransferase)	Glrx1	3.63	3.70
Cell proliferation	NM_013122	Insulin-like growth factor binding protein 2	Igfbp2	2.51	2.78
Cell proliferation	AI101583	Transient receptor potential cation channel, subfamily V, member 6	Trpv6	2.01	2.25
Cell proliferation	BI290527	T-box 2‡	Tbx2	2.66	2.19
Biosynthesis	BE097981	Phosphatidylinositol 4-kinase type 2α	Pi4KII	2.66	3.36
Signal transduction	NM_012707	Glucagon	Gcg	3.07	2.79
Cell growth	AW142962	Prolactin receptor	Prlr	2.22	2.46
Tumor progression	BE102969	Ets variant gene 4 (E1A enhancer binding protein, E1AF)‡	Etv4	2.62	2.25
Tumor progression	BG379319	Transforming growth factor, beta induced	Tgfbi	3.41	2.41
Tumor progression	BE120425	Calcium/calmodulin-dependent protein kinase II gamma	Camk2g	2.17	1.90
Cell cycle	NM_133309	Calpain 8	Capn8	2.06	2.55
Cytoskeleton	BE119221	Actinin, α1	Actn1	2.11	2.09
Downregulated genes (of 53 genes in total)					
Adhesion	AW525315 (AI103913)	Poliovirus receptor-related 3‡	Pvrl3	0.46 (0.44)	0.28 (0.31)
Transcription	NM_013060	Inhibitor of DNA binding 2, dominant negative helix-loop-helix protein	Id2	0.47	0.28
Biosynthesis	NM_022276	Glucosaminyl (*N*-acetyl) transferase 1, core 2	Gcnt1	0.44	0.30
Signal transduction	BI276110	Retinoic acid induced 3‡	Rai3	0.48	0.33
Apoptosis	AI227742	Bcl-2-related ovarian killer protein	Bok	0.44	0.36

Ad, adenomas; Ca, carcinomas; FFCH, focal follicular cell hyperplasias.
†Proliferative lesions were divided into two categories, i.e. FFCH + Ad and Ca.
‡Predicted gene identity.

Table 5. Validation of microarray data by real-time reverse transcription-polymerase chain reaction (PCR)

Gene	FFCH + Ad			Ca		
	Microarray	Real-time PCR normalized by		Microarray	Real-time PCR normalized by	
		Hprt	Gapdh		Hprt	Gapdh
Chi3l1	7.40 ± 1.06*	7.35 ± 2.85***	10.73 ± 4.13	8.67 ± 2.67*	8.14 ± 3.49***	14.09 ± 4.61***
Cp	3.29 ± 0.27**	3.18 ± 0.89****	4.69 ± 1.19****	4.12 ± 0.62**	3.50 ± 0.84****	6.15 ± 0.83****
Slc2a3	2.66 ± 0.25**	2.47 ± 0.66****	3.55 ± 0.93	2.52 ± 0.31**	2.41 ± 0.41****	4.15 ± 0.28***
Scl16a6	2.29 ± 0.53**	2.20 ± 0.73***	3.26 ± 1.12****	2.23 ± 0.26**	2.19 ± 0.63***	3.88 ± 0.89****
Gcg	3.07 ± 0.60*	2.37 ± 0.72***	3.46 ± 0.88	2.96 ± 1.21*	2.55 ± 1.17***	4.40 ± 1.69***
Prlr	2.22 ± 0.61*	1.53 ± 0.36	2.21 ± 0.51****	2.51 ± 0.80**	1.87 ± 0.36***	3.23 ± 0.43****
Pi4KII	2.67 ± 0.89*	2.01 ± 0.74	2.96 ± 1.12****	3.30 ± 0.95**	2.17 ± 0.59***	3.84 ± 0.83****
Actn1	2.13 ± 0.47*	1.61 ± 0.48	2.35 ± 0.73****	2.17 ± 0.82*	1.52 ± 0.38	2.67 ± 0.56****
Pvrl3	0.44 ± 0.07*	0.40 ± 0.08	0.59 ± 0.10****	0.31 ± 0.05*	0.35 ± 0.05***	0.62 ± 0.12****
Rai3	0.48 ± 0.06*	0.42 ± 0.06	0.63 ± 0.09****	0.34 ± 0.08*	0.32 ± 0.06***	0.58 ± 0.17****
Gcnt1	0.44 ± 0.08*	0.63 ± 0.14	0.95 ± 0.17	0.31 ± 0.09*	0.37 ± 0.05***	0.67 ± 0.08****

Gapdh, glyceraldehyde 3-phosphate dehydrogenase; Hprt, hypoxanthine-guanine phosphoribosyltransferase.
Values are mean ± SD ($n = 5$) when the expression level in non-tumor follicles was calculated as 1. A single RNA sample for measurement was an equal mixture of total RNA from the same category tissue preparations from two animals.
*,**: Significantly different from non-tumor follicles at $P < 0.05$ and $P < 0.01$, respectively (Student's *t*-test calculated by GeneSpring).
,*: Significantly different from non-tumor follicles at $P < 0.05$ and $P < 0.01$, respectively (Student's *t*-test).

transcriptional inhibitors of Id family proteins appeared specific. These genes may play stage-dependent roles during carcinogenesis. In particular, selective activation of cell-cycle molecules in the early stages is considered to be essential for lesions to undergo efficient replication in response to TSH-stimulation, and loss of tumor-suppressor functions may be necessary for acquisition of a malignant phenotype during the progression stage. As genes upregulated in common in all types of proliferative lesions, we

doi: 10.1111/j.1349-7006.2009.01094.x

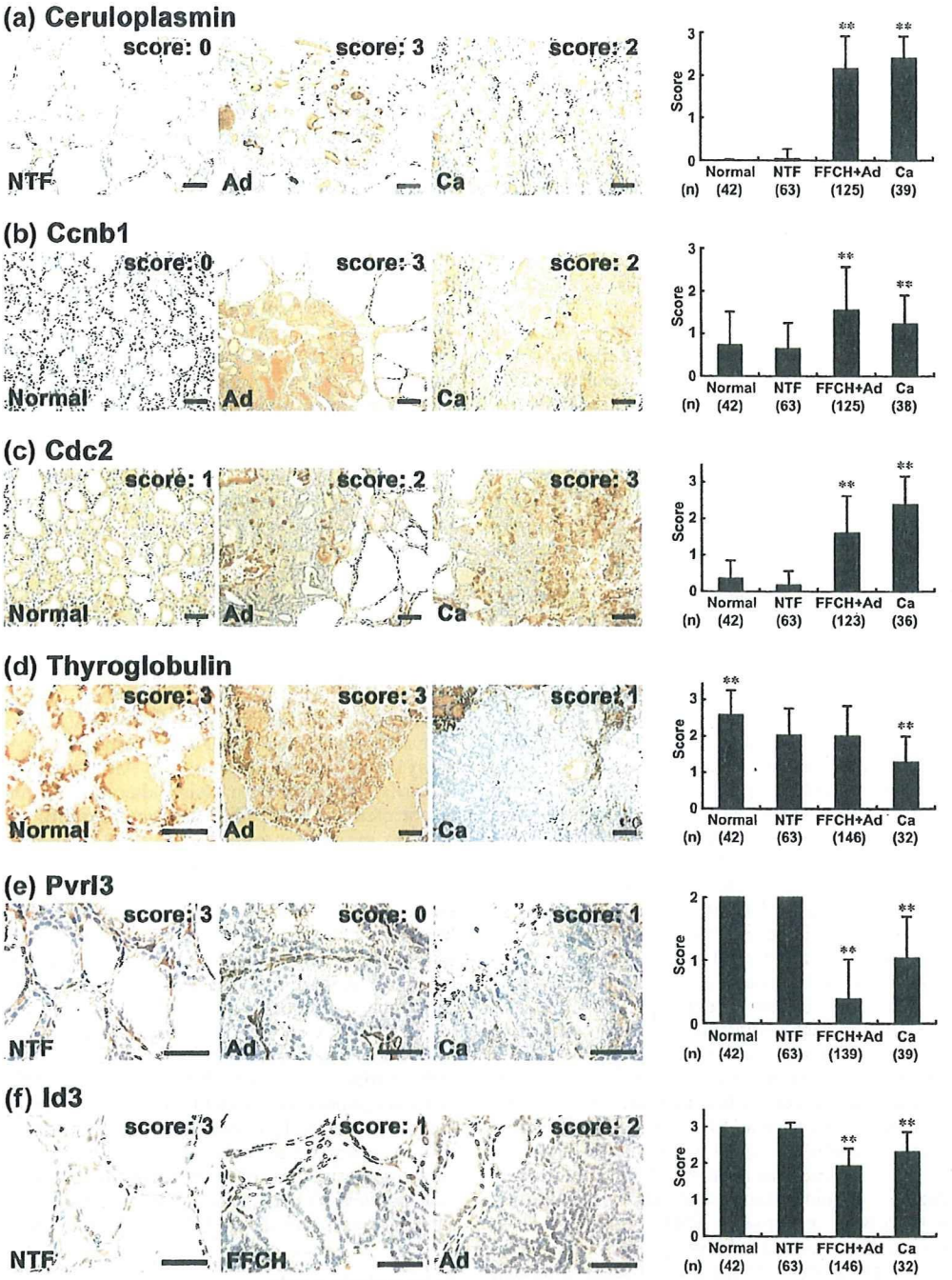

Fig. 2. Immunohistochemical distributions of ceruloplasmin, cyclin B1 (Ccnb1), cell division cycle 2 (Cdc2), thyroglobulin, poliovirus receptor-related 3 (Pvrl3), and inhibitor of DNA binding 3 (Id3) in normal follicular cells of untreated or *N*-bis(2-hydroxypropyl)nitrosamine (DHPN)-treated animals and in proliferative lesions (focal follicular cell hyperplasia [FFCH], adenoma [Ad], carcinoma [Ca]) or surrounding non-tumor follicles (NTF) after promotion with sulfadimethoxine (SDM) for 10 or 15 weeks. (a) Ceruloplasmin in the NTF, Ad, and Ca. Left: NTF nearly lacking ceruloplasmin expression. Middle and right: Ad and Ca showing ceruloplasmin immunoreactivity in the luminal surfaces of cellular membranes of follicular cells. Diffuse or granular immunoreactivity is also evident in the follicular lumina. (b) Ccnb1 in normal follicles, Ad, and Ca. Note fine granular immunoreactivity of Ccnb1 in the cytoplasm of follicular cells. Left: Weak and sparse Ccnb1 localization in normal follicular cells. Middle: Strong and diffuse immunoreactivity in an Ad. Right: Ca demonstrating Ccnb1 immunoreactivity with variable intensity. (c) Cdc2 in normal follicles, Ad, and Ca. Strong Cdc2 immunoreactivity both in the cytoplasm and nucleus of follicular cells. Left: Rather few immunoreactive cells in normal follicles. Middle: An Ad showing sparse Cdc2 immunoreactivity. Right: Note increased numbers of immunoreactive cells in a Ca. (d) Thyroglobulin in normal follicles, Ad, and Ca. Left: Strong and granular thyroglobulin immunoreactivity in the cytoplasm of normal follicular cells as well as diffuse immunoreactivity in the follicular lumina. Middle: Ad showing strong and diffuse thyroglobulin immunoreactivity. Right: A Ca lacking thyroglobulin immunoreactivity in the neoplastic cells. (e) Pvrl3 in the NTF, Ad, and Ca. Left: Diffuse intercellular membrane localization of Pvrl3 in cells comprising NTF. Middle: Ad entirely lacking Pvrl3 expression. Right: Ca showing an irregular and weak intercellular expression pattern. (f) Id3 in NTF, FFCH, and Ad. Left: Diffuse nuclear immunoexpression of Id3 in NTF. Middle: FFCH showing sparse nuclear Id3 expression. Right: Ad showing immunoreactivity in moderate numbers of neoplastic cells. The graphs show scores (mean + SD) for immunohistochemical findings. $^{**}P < 0.01$ versus NTF (Mann–Whitney's *U*-test). (a–f) Scale bar = 50 μm.

also found examples related to cell proliferation, suggesting roles for these molecules consistently throughout carcinogenic processes.

Ceruloplasmin, a copper-containing plasma protein mainly synthesized in the liver, is known to act as a ferroxidase preventing production of toxic Fe and controlling membrane lipid oxidation, while also functioning in angiogenesis and blood coagulation.[19] High levels of antioxidant production likely result from high amounts of reactive oxygen species, which have been implicated in mitogenic signaling and angiogenesis.[27,28] As with high ceruloplasmin levels in the sera of cancer patients, overexpression of ceruloplasmin has been reported in many human malignancies, such as those in the lungs, kidneys, and ovaries.[29–31] With regard to ceruloplasmin in thyroid tumors, it has been demonstrated in follicular cell carcinomas as well as papillary carcinomas, but follicular Ad lack expression.[32–34] In the present study, ceruloplasmin could be immunohistochemically demonstrated in all types of proliferative lesion, in line with transcriptional upregulation. In contrast to the generally benign nature of human Ad, FFCH and Ad in SDM-promoted cases show high cell-proliferation activity similarly to Ca,[9] and this biological behavior may be linked to the increased ceruloplasmin immunoreactivity found in our early proliferative lesions. As discussed by Kondi-Pafiti *et al.*, strong cytoplasmic localization of ceruloplasmin is mainly observed in Ca of human cases, and immunolocalization in luminal secretions (as present in our rat cases) is rare, suggesting a defective catabolism of ceruloplasmin in human Ca.[34]

Cdc2 exerts protein kinase activity by forming complexes with cyclin A2, Ccnb1, and p13suc1 and acts as an active subunit of the M-phase-promoting factor and the M-phase-specific histone H1 kinase.[35] In the present study, increased expression of Ccnb1 and Cdc2, as with other cyclin-related molecules such as cyclin A2, was detected specifically in early proliferative lesions by microarray analysis. Immunohistochemically, we also observed increased expression of Ccnb1 and Cdc2 in both FFCH + Ad and Ca. Chen *et al.* reported coordinated and increased expression of Cdc2 and Ccnb1 in parallel with the pathological grade of human gliomas.[36] They also showed that increased expression of Cdc2 and Ccnb1 contributes to chromosomal instability in tumor cells through alteration of the spindle checkpoint. Thus, the coordinated upregulation of Cdc2 and Ccnb1 observed in the present study might be important as a driving force for both promotion and progression. In another thyroid carcinogenesis study we recently carried out using propylthiouracil as a promoter, a concordant increase of Cdc2 and a cell proliferation marker Ki-67 was found in the proliferative lesions (K. Ago and M. Shibutani, 2008, unpublished data).

Thyroglobulin, a scaffold protein for thyroid hormonogenesis and a storage element for thyroid hormones and iodide, is specifically expressed in the thyroid in response to TSH stimulation.[20] In human malignancies, the presence of thyroglobulin in cancer cells indicates a thyroidal origin.[20] In the present study, although the reason remains unclear, some discrepancy was evident between the mRNA and immunolocalization levels in Ca, the increase in expression on microarray analysis contrasting with the decrease in protein finding. In human thyroid Ca, an inverse relationship between loss of differentiation and thyroglobulin immunoreactivity has been observed, positive cases being less anaplastic,[37] suggesting that the decrease in thyroglobulin in our Ca might have been linked with dedifferentiation, leading to loss of TSH control with malignancy.

Cell adhesion molecules contribute cell-to-cell or cell-to-substratum interactions by homophilic or heterophilic processes.[38] Pvrl molecules, also known as nectins, are adhesion receptors belonging to the IGSF that are involved in cell-to-cell spreading of viruses.[39] Although Pvrl3 protein has not been extensively investigated, it may be a new adhesion molecule expressed on lymphatic endothelial cells.[40] Recent studies have revealed that nectins and nectin-like molecules, in cooperation with integrin and the platelet-derived growth factor receptor, are crucial for mechanisms underlying contact inhibition of cell movement and proliferation.[41] Reduced Pvrl3 expression in all types of proliferative lesions in the present study may reflect acquisition of growth advantage. Interestingly, Pvrl has been shown to be the heterophilic binding partner of another IGSF-type adhesion molecule, tumor suppressor in lung cancer 1 (TSLC1)/IGSF4, a recently identified tumor-suppressor gene.[42,43]

Inhibitor of DNA binding proteins, composed of four members of the helix-loop-helix transcription factors, are known to act as dominant-negative regulators of basic helix-loop-helix transcription factors, and function to inhibit differentiation and enhance cell proliferation.[44,45] In many human malignancies, upregulation of Id has been reported.[46] However, in the present study, all Id isoforms showed downregulation in Ca by microarray analysis, and immunohistochemically, Id3-immunoreactive cells were reduced in all types of proliferative lesions. Similar findings have been reported for human ovarian tumors, in which downregulation of Id3 was noted in 70% of 38 cases.[47] Also, the expression of Id1, Id3, and Id4 was downregulated in microdissected human thyroid Ca compared with surrounding tissues by microarray analysis in one recent study.[48] Although the reason for the inconsistency in the expression alterations between tumor types is not clear, it is possible that gene control mechanisms of Id proteins may differ with the cell type of origin.

In conclusion, we here found differentially regulated genes that may play key roles in early and late stages of thyroid carcinogenesis by microarray analysis of microdissected proliferative lesions developing after promotion with SDM in a two-stage model. Immunohistochemical analysis of representative proliferative lesions indicated facilitation of the cell cycle in early lesions by forming an M-phase promoting factor, as evidenced by the synchronized localization of Ccnb1 and Cdc2, and generation of oxidative stress responses by ceruloplasmin accumulation, as well as reduction of cellular adhesion involving Pvrl3 and cellular differentiation related to transcriptional control by Id3. Decreased expression of thyroglobulin in Ca may reflect dedifferentiation. Although further studies should address particular roles in the processes of thyroid carcinogenesis, the molecules identified in the present study provide pointers to understanding the mechanism of non-genotoxic carcinogenesis and should help in efforts to secure human health.

Acknowledgments

We thank Miss Tomomi Morikawa and Ayako Kaneko for their technical assistance in conducting the animal study. This work was supported by Health and Labour Sciences Research Grants (Research on Food Safety) from the Ministry of Health, Labour, and Welfare of Japan. We all authors disclose here that there are no conflicts of interest that could inappropriately influence the outcome of the present study.

References

1 Thyroid Carcinoma Task Force. AACE/AAES medical/surgical guidelines for clinical practice: management of thyroid carcinoma. American Association of Clinical Endocrinologists. American College of Endocrinology. *Endocr Pract* 2001; **7**: 202–20.

2 Schneider AB, Sarne DH. Long-term risks for thyroid cancer and other neoplasms after exposure to radiation. *Nat Clin Pract Endocrinol Metab* 2005; **1**: 82–91.

3 Kitahori Y, Hiasa Y, Konishi N, Enoki N, Shimoyama T, Miyashiro A. Effect of propylthiouracil on the thyroid tumorigenesis induced by *N*-bis (2-hydroxypropyl) nitrosamine in rats. *Carcinogenesis* 1984; **5**: 657–60.

doi: 10.1111/j.1349-7006.2009.01094.x

4 Jemec B. Studies of the goitrogenic and tumorigenic effect of two goitrogens in combination with hypophysectomy or thyroid hormone treatment. *Cancer* 1980; **45**: 2138–48.
5 Hiasa Y, Ohshima M, Kitahori Y, Yuasa T, Fujita T, Iwata C. Promoting effects of 3-amino-1,2,4-triazole on the development of thyroid tumors in rats treated with *N*-bis (2-hydroxypropyl) nitrosamine. *Carcinogenesis* 1982; **3**: 381–4.
6 Hard GC. Recent developments in the investigation of thyroid regulation and thyroid carcinogenesis. *Environ Health Perspect* 1998; **106**: 427–36.
7 Smith P, Williams ED, Wynford-Thomas D. *In vitro* demonstration of a TSH-specific growth desensitising mechanism in rat thyroid epithelium. *Mol Cell Endocrinol* 1987; **51**: 51–8.
8 Brewer C, Yeager N, Di Cristofano A. Thyroid-stimulating hormone initiated proliferative signals converge *in vivo* on the mTOR kinase without activating AKT. *Cancer Res* 2007; **67**: 8002–6.
9 Mitsumori K, Onodera H, Takahashi M *et al.* Effect of thyroid stimulating hormone on the development and progression of rat thyroid follicular cell tumors. *Cancer Lett* 1995; **92**: 193–202.
10 Roy G, Mugesh G. Bioinorganic chemistry in thyroid gland: effect of antithyroid drugs on peroxidase-catalyzed oxidation and iodination reactions. *Bioinorg Chem Appl* 2006; **2006**: 23214.
11 Shibutani M, Uneyama C, Miyazaki K, Toyoda K, Hirose M. Methacarn fixation: a novel tool for analysis of gene expressions in paraffin-embedded tissue specimens. *Lab Invest* 2000; **80**: 199–208.
12 Uneyama C, Shibutani M, Masutomi N, Takagi H, Hirose M. Methacarn fixation for genomic DNA analysis in microdissected, paraffin-embedded tissue specimens. *J Histochem Cytochem* 2002; **50**: 1237–45.
13 Takagi H, Shibutani M, Kato N *et al.* Microdissected region-specific gene expression analysis with methacarn-fixed, paraffin-embedded tissues by real-time RT-PCR. *J Histochem Cytochem* 2004; **52**: 903–13.
14 Takagi H, Shibutani M, Lee KY *et al.* Impact of maternal dietary exposure to endocrine-acting chemicals on progesterone receptor expression in microdissected hypothalamic medial preoptic areas of rat offspring. *Toxicol Appl Pharmacol* 2005; **208**: 127–36.
15 Shibutani M, Lee KY, Igarashi K *et al.* Hypothalamus region-specific global gene expression profiling in early stages of central endocrine disruption in rat neonates injected with estradiol benzoate or flutamide. *Dev Neurobiol* 2007; **67**: 253–69.
16 Lee KY, Shibutani M, Inoue K, Kuroiwa KUM, Woo GH, Hirose M. Methacarn fixation – effects of tissue processing and storage conditions on detection of mRNAs and proteins in paraffin-embedded tissues. *Anal Biochem* 2006; **351**: 36–43.
17 Hardisty JF, Boorman GA. Thyroid gland. In: Boorman GA, Eustis SL, Elwell MR, Montgomery CA Jr, MacKenzie WF, eds. *Pathology of the Fischer Rat, Reference and Atlas*. San Diego: Academic Press, 1990: 519–36.
18 Imai T, Onose J, Hasumura M, Ueda M, Takizawa T, Hirose M. Sequential analysis of development of invasive thyroid follicular cell carcinomas in inflamed capsular regions of rats treated with sulfadimethoxine after *N*-bis (2-hydroxypropyl) nitrosamine-initiation. *Toxicol Pathol* 2004; **32**: 229–36.
19 Goldstein IM, Kaplan HB, Edelson HS, Weissmann G. Ceruloplasmin. A scavenger of superoxide anion radicals. *J Biol Chem* 1979; **254**: 4040–5.
20 Lin JD. Thyroglobulin and human thyroid cancer. *Clin Chim Acta* 2008; **388**: 15–21.
21 Ziak M, Meier M, Novak-Hofer I, Roth J. Ceruloplasmin carries the anionic glycan oligo/poly α2,8 deaminoneuraminic acid. *Biochem Biophys Res Commun* 2002; **295**: 597–602.
22 Scott IS, Morris LS, Bird K *et al.* A novel immunohistochemical method to estimate cell-cycle phase distribution in archival tissue: implications for the prediction of outcome in colorectal cancer. *J Pathol* 2003; **201**: 187–97.
23 Yamamoto H, Monden T, Ikeda K *et al.* Coexpression of cdk2/cdc2 and retinoblastoma gene products in colorectal cancer. *Br J Cancer* 1995; **71**: 1231–6.
24 Faggiano A, Caillou B, Lacroix L *et al.* Functional characterization of human thyroid tissue with immunohistochemistry. *Thyroid* 2007; **17**: 203–11.
25 Kuramitsu K, Ikeda W, Inoue N, Tamaru Y, Takai Y. Novel role of nectin: implication in the co-localization of JAM-A and claudin-1 at the same cell–cell adhesion membrane domain. *Genes Cells* 2008; **13**: 797–805.
26 Carroll M, Hamzeh M, Robaire B. Expression, localization, and regulation of inhibitor of DNA binding (Id) proteins in the rat epididymis. *J Androl* 2006; **27**: 212–24.
27 Lelkes PI, Hahn KL, Sukovich DA, Karmiol S, Schmidt DH. On the possible role of reactive oxygen species in angiogenesis. *Adv Exp Med Biol* 1998; **454**: 295–310.
28 Suh YA, Arnold RS, Lassegue B *et al.* Cell transformation by the superoxide-generating oxidase Mox1. *Nature* 1999; **401**: 79–82.
29 Stassar MJ, Devitt G, Brosius M *et al.* Identification of human renal cell carcinoma associated genes by suppression subtractive hybridization. *Br J Cancer* 2001; **85**: 1372–82.
30 Hough CD, Cho KR, Zonderman AB, Schwartz DR, Morin PJ. Coordinately up-regulated genes in ovarian cancer. *Cancer Res* 2001; **61**: 3869–76.
31 Wang KK, Liu N, Radulovich N *et al.* Novel candidate tumor marker genes for lung adenocarcinoma. *Oncogene* 2002; **21**: 7598–604.
32 Tuccari G, Barresi G. Immunohistochemical demonstration of ceruloplasmin in follicular adenomas and thyroid carcinomas. *Histopathology* 1987; **11**: 723–31.
33 Song B. Immunohistochemical demonstration of epidermal growth factor receptor and ceruloplasmin in thyroid diseases. *Acta Pathol Jpn* 1991; **41**: 336–43.
34 Kondi-Pafiti A, Smyrniotis V, Frangou M, Papayanopoulou A, Englezou M, Deligeorgi H. Immunohistochemical study of ceruloplasmin, lactoferrin and secretory component expression in neoplastic and non-neoplastic thyroid gland diseases. *Acta Oncol* 2000; **39**: 753–6.
35 Draetta G, Luca F, Westendorf J, Brizuela L, Ruderman J, Beach D. cdc2 protein kinase is complexed with both cyclin A and B. Evidence for proteolytic inactivation of MPF. *Cell* 1989; **56**: 829–38.
36 Chen H, Huang Q, Dong J, Zhai DZ, Wang AD, Lan Q. Overexpression of CDC2/CyclinB1 in gliomas, and CDC2 depletion inhibits proliferation of human glioma cells *in vitro* and *in vivo*. *BMC Cancer* 2008; **8**: 29.
37 Wiseman SM, Griffith OL, Deen S *et al.* Identification of molecular markers altered during transformation of differentiated into anaplastic thyroid carcinoma. *Arch Surg* 2007; **142**: 717–29.
38 Simmons DL. Dissecting the modes of interactions amongst cell adhesion molecules. *Dev Suppl* 1993; **???**: 193–203.
39 Geraghty RJ, Krummenacher C, Cohen GH, Eisenberg RJ, Spear PG. Entry of alphaherpesviruses mediated by poliovirus receptor-related protein 1 and poliovirus receptor. *Science* 1998; **280**: 1618–20.
40 Nelson GM, Padera TP, Garkavtsev I, Shioda T, Jain RK. Differential gene expression of primary cultured lymphatic and blood vascular endothelial cells. *Neoplasia* 2007; **9**: 1038–45.
41 Takai Y, Miyoshi J, Ikeda W, Ogita H. Nectins and nectin-like molecules: roles in contact inhibition of cell movement and proliferation. *Nat Rev Mol Cell Biol* 2008; **9**: 603–15.
42 Murakami Y. Involvement of a cell adhesion molecule, TSLC1/IGSF4, in human oncogenesis. *Cancer Sci* 2005; **96**: 543–52.
43 Wakayama T, Sai Y, Ito A *et al.* Heterophilic binding of the adhesion molecules poliovirus receptor and immunoglobulin superfamily 4A in the interaction between mouse spermatogenic and Sertoli cells. *Biol Reprod* 2007; **76**: 1081–90.
44 Benezra R, Davis RL, Lockshon D, Turner DL, Weintraub H. The protein Id. A negative regulator of helix-loop-helix DNA binding proteins. *Cell* 1990; **61**: 49–59.
45 Ellis HM, Spann DR, Posakony JW. *Extramacrochaetae*, a negative regulator of sensory organ development in *Drosophila*, defines a new class of helix-loop-helix proteins. *Cell* 1990; **61**: 27–38.
46 Sikder HA, Devlin MK, Dunlap S, Ryu B, Alani RM. Id proteins in cell growth and tumorigenesis. *Cancer Cell* 2003; **3**: 525–30.
47 Arnold JM, Mok SC, Purdie D, Chenevix-Trench G. Decreased expression of the *Id3* gene at 1p36.1 in ovarian adenocarcinomas. *Br J Cancer* 2001; **84**: 352–9.
48 Nikolova DN, Zembutsu H, Sechanov T *et al.* Genome-wide gene expression profiles of thyroid carcinoma: Identification of molecular targets for treatment of thyroid carcinoma. *Oncol Rep* 2008; **20**: 105–21.

Supporting Information

Additional Supporting Information may be found in the online version of this article:

Table S1. List of genes showing altered expression in microdissected focal follicular cell hyperplasias (FFCH) + adeomas (Ad) induced in the thyroids of rats using a two-stage thyroid carcinogenesis model (≥2-fold, ≤0.5-fold).

Table S2. List of genes showing altered expression in microdissected carinomas (Ca) induced in the thyroid of rats using a two-stage thyroid carcinogenesis model (≥2-fold, ≤0.5-fold).

Table S3. List of genes showing altered expression in common in all types of thyroid proliferative lesion induced in rats using a two-stage thyroid carcinogenesis model (≥2-fold, ≤0.5-fold).

Please note: Wiley-Blackwell are not responsible for the content or functionality of any supporting materials supplied by the authors. Any queries (other than missing material) should be directed to the corresponding author for the article.

Why Public Health Agencies Cannot Depend on Good Laboratory Practices as a Criterion for Selecting Data: The Case of Bisphenol A

John Peterson Myers,[1] Frederick S. vom Saal,[2] Benson T. Akingbemi,[3] Koji Arizono,[4] Scott Belcher,[5] Theo Colborn,[6] Ibrahim Chahoud,[7] D. Andrew Crain,[8] Francesca Farabollini,[9] Louis J. Guillette Jr.,[10] Terry Hassold,[11] Shuk-mei Ho,[12] Patricia A. Hunt,[11] Taisen Iguchi,[13] Susan Jobling,[14] Jun Kanno,[15] Hans Laufer,[16] Michele Marcus,[17] John A. McLachlan,[18] Angel Nadal,[19] Jörg Oehlmann,[20] Nicolás Olea,[21] Paola Palanza,[22] Stefano Parmigiani,[22] Beverly S. Rubin,[23] Gilbert Schoenfelder,[24] Carlos Sonnenschein,[23] Ana M. Soto,[23] Chris E. Talsness,[25] Julia A. Taylor,[2] Laura N. Vandenberg,[23] John G. Vandenbergh,[26] Sarah Vogel,[27] Cheryl S. Watson,[28] Wade V. Welshons,[29] and R. Thomas Zoeller[30]

[1]Environmental Health Sciences, Charlottesville, Virginia, USA; [2]Division of Biological Sciences, University of Missouri, Columbia, Missouri, USA; [3]Department of Anatomy, Physiology and Pharmacology, College of Veterinary Medicine, Auburn University, Auburn, Alabama, USA; [4]Faculty of Environmental and Symbiotic Science, Prefectural University of Kumamoto, Tsukide, Kumamoto, Japan; [5]Department of Pharmacology and Cell Biophysics, Center for Environmental Genetics, University of Cincinnati, Cincinnati, Ohio, USA; [6]The Endocrine Disruption Exchange, Paonia, Colorado, USA; [7]Institut für Klinische Pharmakologie und Toxikologie Charité, Universitätsmedizin Berlin, Campus Benjamin Franklin, Berlin, Germany; [8]Department of Biology, Maryville College, Maryville, Tennessee, USA; [9]Dipartimento di Fisiologia, Università di Siena, Siena, Italy; [10]Department of Zoology, University of Florida, Gainesville, Florida, USA; [11]School of Molecular Biosciences, Washington State University, Pullman, Washington, USA; [12]Department of Environmental Health, University of Cincinnati, Cincinnati, Ohio, USA; [13]National Institutes of Natural Science, Okazaki Institute for Integrative Bioscience, Bioenvironmental Science, Okazaki, Japan; [14]Department of Biological Sciences, Brunel University, Uxbridge, United Kingdom; [15]Division of Cellular and Molecular Toxicology, National Institute of Health Sciences, Tokyo, Japan; [16]Department of Molecular and Cell Biology, University of Connecticut, Storrs, Connecticut, USA; [17]Department of Epidemiology, Rollins School of Public Health, Emory University, Atlanta, Georgia, USA; [18]Center for Bioenvironmental Research, Tulane and Xavier Universities, New Orleans, Louisiana, USA; [19]Instituto de Bioingeniería and CIBERDEM, Universidad Miguel Hernández de Elche, Alicante, Spain; [20]Goethe University Frankfurt am Main, Department Aquatic Ecotoxicology, Frankfurt, Germany; [21]Hospital Clínico, CIBERESP, University of Granada, Granada, Spain; [22]Dipartimento di Biologia Evolutiva e Funzionale, Universita' di Parma, Parma, Italy; [23]Tufts Medical School, Boston, Massachusetts, USA; [24]Institute of Pharmacology and Toxicology, University of Wuerzburg, Wuerzburg Germany; [25]Charité University Medical School Berlin, Berlin, Germany; [26]Department of Biology, North Carolina State University, Raleigh, North Carolina, USA; [27]Chemical Heritage Foundation, Philadelphia, Pennsylvania, USA; [28]Biochemistry and Molecular Biology, University of Texas Medical Branch, Galveston, Texas, USA; [29]Department of Biomedical Sciences, University of Missouri, Columbia, Missouri, USA; [30]Biology Department, University of Massachusetts, Amherst, Massachusetts, USA

BACKGROUND: In their safety evaluations of bisphenol A (BPA), the U.S. Food and Drug Administration (FDA) and a counterpart in Europe, the European Food Safety Authority (EFSA), have given special prominence to two industry-funded studies that adhered to standards defined by Good Laboratory Practices (GLP). These same agencies have given much less weight in risk assessments to a large number of independently replicated non-GLP studies conducted with government funding by the leading experts in various fields of science from around the world.

OBJECTIVES: We reviewed differences between industry-funded GLP studies of BPA conducted by commercial laboratories for regulatory purposes and non-GLP studies conducted in academic and government laboratories to identify hazards and molecular mechanisms mediating adverse effects. We examined the methods and results in the GLP studies that were pivotal in the draft decision of the U.S. FDA declaring BPA safe in relation to findings from studies that were competitive for U.S. National Institutes of Health (NIH) funding, peer-reviewed for publication in leading journals, subject to independent replication, but rejected by the U.S. FDA for regulatory purposes.

DISCUSSION: Although the U.S. FDA and EFSA have deemed two industry-funded GLP studies of BPA to be superior to hundreds of studies funded by the U.S. NIH and NIH counterparts in other countries, the GLP studies on which the agencies based their decisions have serious conceptual and methodologic flaws. In addition, the U.S. FDA and EFSA have mistakenly assumed that GLP yields valid and reliable scientific findings (i.e., "good science"). Their rationale for favoring GLP studies over hundreds of publically funded studies ignores the central factor in determining the reliability and validity of scientific findings, namely, independent replication, and use of the most appropriate and sensitive state-of-the-art assays, neither of which is an expectation of industry-funded GLP research.

CONCLUSIONS: Public health decisions should be based on studies using appropriate protocols with appropriate controls and the most sensitive assays, not GLP. Relevant NIH-funded research using state-of-the-art techniques should play a prominent role in safety evaluations of chemicals.

KEY WORDS: bisphenol A, endocrine disruptors, FDA, Food and Drug Administration, GLP, good laboratory practices, low-dose, nonmonotonic, positive control. *Environ Health Perspect* 117:309–315 (2009). doi:10.1289/ehp.0800173 available via *http://dx.doi.org/* [Online 22 October 2008]

Regulatory agencies in the United States and the European Union (EU) have justified the decision to declare the estrogenic chemical bisphenol A (BPA) safe at current levels of human exposure based on a few studies conducted using Good Laboratory Practices (GLP). In contrast, these agencies have rejected for consideration in their risk assessment of BPA hundreds of laboratory animal and mechanistic cell culture studies conducted by academic and government scientists reporting harm at very low doses of BPA. These studies were rejected primarily because they were not conducted using GLP. We suggest that decisions based on this logic are misguided and will result in continued risk to public health from exposure to BPA, as well as other manmade chemicals.

GLP is a federal rule for conducting research on the health effects or safety testing of drugs or chemicals submitted by private research companies for regulatory purposes. The GLP outlines basic guidelines for conducting scientific research, including the care and feeding of laboratory animals, standards for facility maintenance, calibration and care of equipment, personnel requirements, inspections, study protocols, and collection and storage of raw data (Goldman 1988). These regulations were developed in response to widespread misconduct by private research companies; this misconduct was possible because their data usually do not go through the rigorous, multistage scientific review that is normal for academic data funded by federal agencies and published in the peer-reviewed literature. The lack of these safeguards from academic science had enabled fraud. The U.S. Food and Drug

Address correspondence to J.P. Myers, Environmental Health Sciences, 421 Park St., Charlottesville, VA 22902 USA. Telephone: (434) 220-0348. Fax: (434) 220-0347. E-mail: jpmyers@ehsic.org

The authors declare they have no competing financial interests.

Received 9 September 2008; accepted 22 October 2008.

Administration (U.S. FDA) first issued rules for GLP in 1978 after a 2-year federal investigation into sloppy laboratory practices of a number of private research companies (Lublin 1978; Markowitz and Rosner 2002). What began as serious concerns about poor quality research expanded into a criminal investigation of Industrial Bio-Test (IBT), one of the largest private laboratories at the time and a subsidiary of Nalco Chemical Company. In response to the federal investigation, the U.S. Environmental Protection Agency (EPA) demanded that 235 chemical companies re-examine the > 4,000 tests conducted by the laboratory. In 1983, three men from IBT were found guilty of deliberating doctoring data and were sentenced to prison (Lublin 1978; Markowitz and Rosner 2002). The fraudulent practices of IBT brought into question 15% of the pesticides approved for use in the United States. That same year, the U.S. EPA issued similar GLP rules for regulatory testing.

Both the U.S. FDA (2008a) and European Food Safety Authority (ESFA 2006) have recently published documents demonstrating that their decision to continue to declare BPA safe at current exposure levels was based primarily on the results of a few industry-funded studies that followed GLP guidelines. These decisions stand in stark contrast to the decisions concerning the potential risks to human health reached by a panel of 38 experts at a U.S. National Institutes of Health (NIH)-sponsored conference, who published The Chapel Hill Consensus Statement (vom Saal et al. 2007), as well as five review articles (Crain et al. 2007; Keri et al. 2007; Richter et al. 2007a; Vandenberg et al. 2007a; Wetherill et al. 2007). These peer-reviewed articles covered approximately 700 articles concerning BPA and represented a comprehensive review of the literature as of the end of 2006. In addition, the U.S. FDA draft decision contradicted the conclusions reached by the National Toxicology Program (NTP), which had spent 2 years investigating this question (NTP 2008). An important role of the NTP is to advise the U.S. FDA about the science relating to toxic chemicals in food, but in an unusual move, the U.S. FDA chose to release its draft report before the release of the final report on BPA by the NTP and without indicating who at the U.S. FDA was involved in preparing the draft report (U.S. FDA 2008b). At a hearing on 16 September 2008 regarding the draft report on BPA, the U.S. FDA announced that their goal was to have a subcommittee of the U.S. FDA Science Board complete a review of the draft decision by the end of October 2008. This would presumably also involve review by the subcommittee members of the approximately 1,000 articles relating to BPA.

We believe that the methods employed in chemical industry–sponsored GLP studies are incapable of detecting low-dose endocrine-disrupting effects of BPA and other hormonally active chemicals. Detecting endocrine-disrupting effects at low doses of chemicals such as BPA requires sophisticated and modern assays and analyses that have been developed in advanced, usually federally funded laboratories over the past decade. This is especially apparent when one examines what is now known about functional effects of BPA on a wide range of end points (Richter et al. 2007a; Welshons et al. 2006; Wetherill et al. 2007). These end points include those mediated by recently discovered estrogen response pathways initiated in human and animal cell membranes (nonclassical or alternative estrogen response mechanisms), which multiple laboratories have shown to be equally sensitive to BPA and estradiol in terms of activating effects in human and animal cells at low picomolar through low nanomolar concentrations (Alonso-Magdalena et al. 2008; Wetherill et al. 2007; Wozniak et al. 2005; Zsarnovszky et al. 2005).

The effects of BPA documented in these studies include a diverse array for which there are no data from GLP studies because the end points have not been examined: altered metabolism related to metabolic syndrome (Alonso-Magdalena et al. 2005, 2006, 2008; Ropero et al. 2008); altered adiponectin secretion (Hugo et al. 2008), which is a condition predicting heart disease and type 2 diabetes (Lang et al. 2008); altered epigenetic programming leading to precancerous lesions of the prostate (Ho et al. 2006); differential growth patterns in the developing prostate (Timms et al. 2005); abnormal growth, gene expression, and precancerous lesions of the mammary glands (Soto et al. 2008); and adverse effects on the female reproductive system, including uterine fibroids, paraovarian cysts, and chromosomal abnormalities in oocytes (Newbold et al. 2007; Susiarjo et al. 2007). There is also a large literature on neuroanatomic, neurochemical, and behavioral abnormalities caused by low doses of BPA (Leranth et al. 2008; Richter et al. 2007a), which also are not capable of being detected by current GLP studies conducted for regulatory purposes because of their out-of-date assays.

The approaches used by academic and government scientists to study the potential health hazards of BPA contrast sharply with those still used by the chemical industry that are relied on by regulatory agencies in the United States and Europe, including the two studies identified by both the U.S. FDA and European Food Safety Authority (EFSA) as central to the decision to declare BPA safe at current human exposure levels (Tyl et al. 2002, 2008a). By using outdated and insensitive assays that were supposed to have been replaced by a new battery of screens and tests by 2000 [as mandated by the U.S. Congress in 1996 in the Food Quality Protection Act (1996), but which has, as yet, still not occurred], these studies conducted using GLP fail to find any adverse effects.

Reliability and Validity

Reliability and validity are separate issues, although in the experimental research described here, validity and reliability basically refer to research that is credible. Golafshani (2003) noted that "reliability" refers to the extent to which results are consistent over time and are an accurate representation of the total population under study. Of central importance is that the results of a study must be reproduced under a similar methodology to be considered to be reliable. "Validity" refers to whether the research measures what it was intended to measure, and valid findings are considered to be true. In other words, reliability is determined by whether the results are replicable, whereas validity is assessed by whether the methods used result in finding the truth as a result of the investigator actually measuring what the study intended to measure.

Use of GLP in Regulatory Decision Making

Despite strong evidence of aberrations caused by low doses of BPA in animals exposed during fetal and neonatal life in studies conducted by the world's leading academic and government experts in the fields of endocrine disruption, endocrinology, neurobiology, reproductive biology, genetics, and metabolism, a relatively small number of studies reporting no adverse effects at low doses of BPA have continued to be promoted by the chemical industry and used by regulatory agencies (e.g., Ashby et al. 1999; Cagen et al. 1999; Tyl et al. 2002, 2008a). According to the U.S. FDA, these are accepted because they used GLP (U.S. EPA 2008), with the implication that studies not employing GLP are not reliable or valid (U.S. FDA 2008a).

GLP does not guarantee reliability or validity of scientific results. Unfortunately, although GLP creates the semblance of reliable and valid science, it actually offers no such guarantee. GLP specifies nothing about the quality of the research design, the skills of the technicians, the sensitivity of the assays, or whether the methods employed are current or out-of-date. (All of the above are central issues in the review of a grant proposal by an NIH panel.) GLP simply indicates that the laboratory technicians/scientists performing experiments follow highly detailed U.S. EPA requirements [or in the EU, Organization for Economic Co-operation and Development (OECD) requirements] for record keeping, including details of the conduct of the

experiment and archiving relevant biological and chemical materials (U.S. EPA 2008).

These record-keeping procedures in GLP were instituted because of widespread misconduct being committed by commercial testing laboratories (described above). These fraudulent results were possible because contract laboratory studies used in the regulatory process are rarely subject to the checks and balances that peer-reviewed, replicated scientific findings undergo. Without that acid test of reliability (replication by other independent scientists), other procedures were needed. Hence GLP was implemented, despite its severe limitations.

NIH-funded research subject to more stringent reviews than GLP. Although few NIH-funded investigators adhere to GLP-mandated record keeping, the procedures of GLP are actually surpassed by the procedures required for NIH-funded science published in peer-reviewed journals. NIH-funded studies pass through three phases of peer review that are far more challenging than GLP requirements. First, the principal scientists must have demonstrated competence to conduct the research, and experimental methods, assays, and laboratory environment must involve use of state-of-the-art techniques to be competitive for NIH funding. Second, results are published in peer-reviewed journals, with detailed evaluations by independent experts examining all aspects of the study. And third, the findings are challenged by independent efforts to replicate; for example, the initial findings concerning the stimulating effects of estrogenic chemicals on the mouse prostate (Nagel et al. 1997; vom Saal et al. 1997) were independently replicated and extended by Gupta (2000), which led to an editorial identifying "initial results confirmed" (Sheehan 2000).

Typically, within a laboratory, interesting findings are also followed by subsequent publications extending the prior findings; examples include the findings of BPA effects on β cells in the mouse pancreas (Alonso-Magdalena et al. 2005, 2006, 2008) and the effects of estrogenic chemicals and drugs on the developing mouse prostate that followed earlier findings (described above) from this same group (Timms et al. 2005; Richter et al. 2007b). In particular, independent replication by competent, respected scientists is the main criterion of acceptance of the findings as having been demonstrated to be reliable and having been validated by virtue of coming to the same conclusion using a variety of sophisticated techniques in multiple publications.

An important criticism of the approach taken by the U.S. FDA in its assessment of the now approximately 1,000 articles on BPA is that it appears to have made no attempt to connect the dots between replicated studies; instead, the U.S. FDA appears to have assessed each study without regard to whether it had been confirmed by other studies.

Thus, collectively, many phases used to verify the reliability and validity of NIH-funded published research have been completely ignored by the U.S. FDA, whereas industry-funded GLP research is rarely, if ever, subject to these central requirements and yet is accepted by regulatory agencies as reliable and valid.

The U.S. FDA's misguided gold standard. In this light, the U.S. FDA's reliance upon GLP as the gold standard is scientifically misguided. Furthermore, U.S. FDA administrators are ignoring published critiques of the GLP studies it considers reliable and valid, such as the study by Tyl et al. (2002) and two coordinated studies conducted at the same time by Ashby et al. (1999) and Cagen et al. (1999). Each was an industry-funded study conducted using GLP. Each was harshly criticized in peer-reviewed publications by academic scientists and government panels [Center for the Evaluation of Risks to Human Reproduction (CERHR) 2007; NTP 2001; vom Saal and Hughes 2005; vom Saal and Welshons 2006]. Yet, the U.S. FDA and EFSA panels still assert that these studies represent the gold standard in toxicologic research.

Specifically, the studies of Cagen et al. (1999) and Ashby et al. (1999) were recently rejected by the NTP CERHR panel on BPA as unusable for consideration in its evaluation of the health hazards posed by BPA (CERHR 2007). Both the Ashby et al. (1999) and Cagen et al. (1999) studies reported finding no effect of their positive control [the estrogenic drug diethylstilbestrol (DES)] on any outcome, although these failures were not acknowledged by the authors in either article. In experimental science, the failure of a positive control to show an effect indicates the experiment failed, which is the conclusion reached by the CERHR panel (CERHR 2007).

The Tyl et al. 2002 study, which the U.S. FDA still accepts as a major study for determination of the safety of BPA (U.S. FDA 2008a, 2008b), was criticized by an NTP panel that met in 2000 to examine the low-dose issue (NTP 2001), as well as in subsequent publications (vom Saal and Hughes 2005; vom Saal and Welshons 2006), for using an insensitive rat (the CD-SD rat) that requires extremely high doses (≥ 50 μg/kg/day) of the potent estrogenic drug ethinylestradiol to show effects such as those examined in the study by Tyl et al. (2002). This dose of ethinylestradiol is > 100 times higher than the approximately 0.3 μg/kg/day used by women in oral contraceptives. The fact that Tyl et al. (2002) adhered to GLP did not protect them from using insensitive animals. This led the NTP (2001) to state:

> Because of clear species and strain differences in sensitivity, animal model selection should be based on responsiveness to endocrine-active agents of concern (i.e., responsive to positive controls), not on convenience and familiarity.

Thus, when reviewed by other scientists, three prior major GLP studies of BPA have been found to be so flawed as to be useless for guiding regulatory agencies in decision making. A new GLP study has now been published by Tyl et al. (2008a). Close examination of this study also reveals fatal flaws which render it useless for regulatory purposes, even though it conforms to GLP.

Examples of Flaws Ignored by the U.S. FDA and EFSA in a Recent GLP Study of BPA

In summary, the flaws in Tyl et al. (2008a) are as follows:

- The high dose required for the positive control (estradiol) to cause an effect means the system used by Tyl et al. (2008a), at least in her laboratory, is relatively insensitive to exogenous estrogens and thus inappropriate for studying low-dose effects of estrogenic compounds such as BPA. The lack of response to low doses of estradiol or BPA in the Tyl laboratory is puzzling, in that the strain of mice used in these experiments (the CD-1 mouse) has been reported in > 20 other peer-reviewed publications to show adverse effects in response to very low doses of BPA (vom Saal 2008), as well as many other studies showing low-dose effects in response to the natural hormone estradiol, the estrogenic drugs ethinylestradiol and DES, and to other estrogenic chemicals.
- Tyl et al. (2008a) used insensitive, out-of-date protocols and assays that are incapable of finding many of the adverse effects reported by more sophisticated studies conducted by independent NIH-funded scientists as well as scientists funded by government agencies in other countries.
- In the specific case of testing for changes in prostate weight, Tyl et al. (2008a) reported an abnormally high prostate weight for control animals that exceeds by > 70% the prostate weights reported by other studies for animals of the same strain and similar age (e.g., Gupta 2000; Ruhlen et al. 2008). This suggests that the dissection procedures for the prostate in the Tyl laboratory included other nonprostatic tissues in the weight measurements, rendering them unusable for studying weight changes in the prostate in response to BPA or estradiol; neither chemical showed any effect on the selected end points, which directly contradicts other findings concerning opposite effects of low and high doses of estrogen on the prostate (Putz et al. 2001; Timms et al. 2005; vom Saal et al. 1997).

Aberrant insensitivity of CD-1 mouse to estrogens. Tyl et al. (2008a) used estradiol as a positive control. It was fed to female mice before and during pregnancy and lactation at 80–220 μg/kg/day; after weaning, estradiol was fed to offspring at doses of 80–100 μg/kg/day. Estradiol was used as a positive control because BPA is a man-made endocrine-disrupting estrogenic chemical.

Many published findings reporting effects of very low doses of positive control estrogens and BPA in CD-1 mice demonstrate that the CD-1 mouse was somehow rendered insensitive in the test system used by Tyl et al. (2008a). The fact that a dose of 100–200 μg/kg/day estradiol was necessary to show an effect of the positive control predicts that Tyl et al. (2008a) should not detect effects of BPA < 10–100 mg/kg/day, far above the low-dose range relevant to human exposures that was supposedly of interest.

For nuclear estrogen receptor–mediated effects via regulation of gene activity (nuclear estrogen receptors are transcription factors whose activity is regulated by binding to estrogen), prior studies have typically shown a 1,000-fold lower activity for BPA relative to estradiol or potent estrogenic drugs, including DES and ethinylestradiol. For example, Richter et al. (2007b) reported an increase in androgen receptor gene activity to estradiol at 1 pM (0.28 pg/mL) in fetal CD-1 mouse prostatic mesenchyme cells in primary culture, and the same response was found for BPA at 1,000 pM (228 pg/mL); the *in vitro* response to estradiol was predicted by the response of the prostate to increasing free serum estradiol from 0.2 to 0.3 pg/mL in male mouse fetuses via estradiol administration to the mother (vom Saal et al. 1997). Other research showed that a significant effect on development of the male reproductive system in CF-1 mice occurred at a maternal dose of 0.002 μg/kg/day ethinylestradiol (Thayer et al. 2001), similar to effects observed with 2–20 μg/kg/day BPA (vom Saal et al. 1998). The research of Honma et al. (2002) showed accelerated puberty in CD-1 (ICR) mice at a DES dose of 0.02 μg/kg/day (the positive control), and the same response to BPA occurred at 20 μg/kg/day, again revealing a 1,000-fold difference between the positive control estrogen and BPA.

There are many other examples of findings where a higher dose of BPA was required to cause the same effect as the positive control estrogen (estradiol, ethinylestradiol, or DES) in studies where the effects were mediated by the classical nuclear estrogen receptors, in contrast to the more recently discovered rapid signaling estrogen response system where BPA and these positive control estrogens have equal potency, as described above. In summary, CD-1 mice have been used by a large number of academic and government investigators and have been reported in peer-reviewed publications to be sensitive to positive control estrogens within the range of human sensitivity based on *in vivo* and *in vitro* studies via the classical estrogen receptor α–mediated response mechanism. The CD-1 mouse is the animal model that has been used by the U.S. National Institute of Environmental Health Sciences (NIEHS) for decades, because it is considered the best animal model for predicting the effects of developmental exposure to estrogen in humans (Newbold 1995; Newbold et al. 2007).

The failure of traditional toxicologic studies conducted by Tyl et al. (2008a, 2008b) to detect the wide range of adverse effects of even relatively high doses of BPA or of low doses of estradiol that have been reported in numerous studies by academic and government scientists provides evidence that the GLP protocols established long ago by regulatory agencies to determine the toxicity of chemicals are inappropriate for detecting the endocrine-disrupting activities of chemicals such as BPA. Indeed, this was the premise of the congressional mandate in the Food Quality Protection Act (1996) for the U.S. EPA to establish a new set of assays for endocrine-disrupting chemicals, although this process has been systematically delayed and is > 8 years behind the congressionally mandated date of 2000 to have these new assays validated.

Citing Tyl et al. (2008a), the EFSA report on BPA (EFSA 2006) stated that "the positive control substance, 17β-estradiol, resulted in reproductive and developmental toxicity." This report failed to acknowledge that only a very high dose of the positive control was sufficient to elicit effects and that this meant that the experiments conducted in the Tyl laboratory were for some reason very insensitive to any estrogen and thus inappropriate for use in a study to examine low-dose estrogenic effects of BPA.

Based on the preliminary report released by the U.S. FDA regarding BPA (U.S. FDA 2008a), it appears that the U.S. FDA has followed the lead of the EFSA in its lack of understanding of the importance of the dose of the positive control estrogen required to cause adverse effects. The consequence is that the U.S. FDA has relied primarily on the study of Tyl et al. (2008a, 2008b), with the result that the U.S. FDA has assured Americans that BPA is safe at current human exposure levels.

Several factors might account for the insensitivity of the CD-1 mouse in the Tyl et al. studies (2008a, 2008b) conducted at Research Triangle Institute (RTI), a testing facility that conducted these (as well as previous) studies funded by the American Chemistry Council. One possibility is that the diet used in these studies may have interfered with the results. The feed used by Tyl et al. (2008a) in this experiment (Purina 5002) has been shown by others to interfere with responses to exogenous estrogenic chemicals, blocking adverse effects documented on other diets. For example, a number of years ago, Thigpen et al. (2003) at the NIEHS recommended against the use of Purina 5002 in studies of endocrine-disrupting chemicals. Tyl et al. (2008a) measured some specific phytoestrogens in Purina 5002 feed by chemical analysis; however, in a report on NIH-sponsored meetings on this subject, Heindel and vom Saal (2008) pointed out that this is an insufficient control for total dietary estrogenic contaminants that can disrupt studies involving the effects of estrogenic chemicals.

A second possibility is that there are strain differences in sensitivity developed in the CD-1 mouse sold by the various Charles River Laboratories located in different regions. We consider this unlikely, because most laboratories regularly replace their CD-1 mouse breeder stock from Charles River Laboratories, and practices there make it unlikely that the sensitivity of this outbred stock to estrogens has changed dramatically over a very short period of time. Also, because RTI, where the Tyl studies were conducted, is very near the laboratories of the NIEHS, it is likely that the CD-1 mice used by these two programs were purchased from the same breeding facility.

Use of insensitive, out-of-date protocols and assays. Another serious concern about the two recent studies by Tyl et al. (2008a, 2008b) is the experimental approach used, thus raising questions about the validity of the studies. The study design used by Tyl et al. (2008a, 2008b) has been superseded by advances in both experimental design and analytical tools developed by NIH-funded scientists (and their counterparts in Europe and Asia) since the mid-1990s. The methods used by Tyl et al., primarily wet weight changes of tissues, gross histologic changes, and developmental landmarks such as vaginal opening, were established procedures by the 1950s. Thus, a major limitation of the Tyl studies is the failure to measure more meaningful and sensitive end points in order to detect the effects of low-dose BPA exposure, which are often not macroscopic in nature. Indeed, in 2001, the director of the reproductive division of the National Health and Environmental Effects Research Laboratory at the U.S. EPA stated that the inconclusive results concerning effects of BPA on reproductive toxicology can only be solved by understanding the mechanisms (Triendl 2001). With current GLP standards it is not possible to study mechanisms because they still rely on out-of-date assays.

As one example of a comparison between the approach by Tyl et al. (2008a) and independent government-funded academic scientists, extensive research has been conducted by Soto et al. (2008) and by other independent academic and government scientists

describing effects of exposure of female mice and rats to very low doses of BPA during perinatal development on the mammary glands (Jenkins et al. 2009). Although Tyl et al. (2008a) reported no low-dose effects of BPA on the mammary glands using conventional histologic analysis, there have been consistent findings of adverse effects of low doses of BPA from studies that used more sophisticated and sensitive analysis of whole mounted mammary glands to facilitate detection of microscopic lesions, coupled with immunostaining for regulatory proteins as well as techniques for determination of aberrant gene expression associated with progression to cancer. These peer-reviewed studies have reported detecting changes during embryonic development of mammary glands as well as abnormalities detected during adolescence through adulthood that are indicative of mammary gland cancer as well as other developmental abnormalities (Colerangle and Roy 1997; Durando et al. 2007; Jenkins et al. 2009; LaPensee et al. 2008; Markey et al. 2001, 2005; Moral et al. 2008; Munoz-de-Toro et al. 2005; Murray et al. 2007; Nikaido et al. 2004; Vandenberg et al. 2006, 2007b; Wadia et al. 2007).

Similar to the findings for the mammary gland, Ogura et al. (2007) reported that if tissues were analyzed by conventional histologic methods (staining with hematoxalin and eosin), prenatal exposure to low doses of BPA or DES showed no effects on prostate development, whereas if the sections were analyzed using antibodies that identified basal cells and basal cell squamous metaplasia, then significant effects were revealed. Squamous metaplasia of basal cells indicates abnormal proliferation and function of the prostate stem cell population that is thought to transform into neoplastic cells; Ho et al. (2006) reported that neonatal exposure to very low doses of BPA caused 100% of male rats to develop high-grade prostatic intraepithelial neoplastic lesions later in life. All of these studies were rejected by the U.S. FDA as not adequate for making regulatory decisions about the safety of BPA. Instead, the U.S. FDA relied upon Tyl et al. (2008a), even though the study used techniques that Ogura et al. (2007) showed lacked the sensitivity of 21st century experimental approaches.

Although findings regarding changes in brain structure, brain chemistry, and behavior represent the largest portion of the literature on low-dose BPA, Tyl et al. (2008a) did not examine any neurobehavioral end points. The NTP (2008) and the NIEHS conference consensus reports (vom Saal et al. 2007) both indicated concern about neurobehavioral effects of low doses of BPA. Thus, the absence of studies that included neurobehavioral end points is a glaring omission of Tyl et al. (2008a, 2008b).

Flawed prostate dissection. Data presented by Tyl et al. (2008a) raise questions about the adequacy of techniques used in their BPA studies. Specifically, Tyl et al. (2008a) reported that the prostate in 3.5-month-old control male CD-1 mice weighed > 70 mg [see Table 3 in Tyl et al. (2008a) for data on F_1 retained males]. This average control weight contrasts sharply with those reported from other laboratories. Specifically, the weight of the prostate in 2- to 3-month-old CD-1 mice using the dissection technique based on both Ruhlen et al. (2008) and Gupta (2000) and at the NIEHS (Newbold RR, personal communication) is about 40 mg. Several studies have reported that prenatal exposure to very low doses of BPA and positive control estrogens increased prostate size, prostatic androgen receptors, and prostate androgen receptor gene activity (Gupta 2000; Richter et al. 2007b; Thayer et al. 2001; Timms et al. 2005; vom Saal et al. 1997), but the enlarged prostate of experimental animals exposed to BPA in these laboratories weighed less than the prostates in the control animals of Tyl et al. (2008a). This raises serious questions about the procedures and/or animals used by Tyl et al. The weight of prostate reported by Tyl et al. (2008a) suggests that the technique used for dissecting the prostate resulted in nonprostatic tissue being weighed along with prostate. The seminal vesicle, coagulating gland, and dorsolateral prostate all merge together where the ejaculatory ducts enter the urethra, and there are also fat deposits on the prostate. This poses a challenge for those without proper training in distinguishing these different tissues during dissection in mice.

Alternatively, as male rodents age, they are prone to develop prostatitis. Although this inflammatory disease leads to an increase in prostate size and could thus account for the very large prostate weights reported by Tyl et al. (2008a), anyone familiar with the appearance of prostatitis would detect this abnormality upon histologic examination, which Tyl et al (2008a) supposedly conducted. Also, prostatitis is rare in young-adult mice or rats (Cowin et al. 2008), and the size of the prostates in the Tyl et al. (2008a) study were similar to those for middle-aged and old male mice.

The findings regarding effects of BPA on the prostate presented by Tyl et al. (2008a) are thus suspect and cannot be used as evidence that other earlier studies (Gupta 2000; Timms et al. 2005; vom Saal et al. 1997) are not replicable. Given these problems in prostate weight measurements, it is not surprising that even very high doses of BPA or estradiol reported by Tyl et al. (2008a) had no effect on the prostate, in sharp contrast to other studies that showed stimulation of the prostate at low doses of estrogen and inhibition at high doses (Putz et al. 2001; Timms et al. 2005).

In addition to the problem associated with the high prostate weight reported by Tyl et al. (2008a), in a separate measurement the authors combined the anterior prostate (coagulating gland) and seminal vesicle, presenting these two organs as one combined outcome measure. This is wrong and misleading. The coagulating glands emerge as the anterior ducts of the prostate from the dorsocranial region of the urogenital sinus, whereas the seminal vesicles bud from the proximal region of the Wolffian ducts. Elevated estrogen is associated with an increase in prostate size associated with an increase in prostate androgen receptors, whereas a decrease in seminal vesicle size is associated with a reduction in 5α-reductase, an enzyme that converts testosterone to the more potent androgen 5α-dihydrotestosterone (Nonneman et al. 1992). Low doses of BPA have been shown to decrease the size of organs that differentiate from the embryonic Wolffian ducts (epididymides and seminal vesicles) while increasing the size of regions of the prostate that develop from the urogenital sinus (vom Saal et al. 1998). Combining these different organs (it is technically not difficult to separate them) was thus inappropriate because they develop from different embryonic tissues that show markedly different responses to estrogenic chemicals during development. In fact, Ogura et al. (2007) reported that the anterior prostate (coagulating glands) showed the greatest expression of ER-α, and also showed the most pronounced indication of basal cell squamous metaplasia in response to developmental exposure to low doses of DES and BPA relative to other regions of the prostate.

Conclusions

Because the control data of Tyl et al. (2008a) were not consistent with the prior published literature for prostate weight of young-adult CD-1 male mice and because their methods were inappropriate for revealing an extensive body of adverse effects detected using more sophisticated approaches, we deem the findings by Tyl et al. to be invalid. Hundreds of studies show adverse effects of BPA in animals, with many conducted at concentrations equivalent to current human levels of BPA exposure; thus, it is unlikely that academic scientists would bother to replicate the outdated approaches used by Tyl et al. (2008a, 2008b). This lack of replication is typical of GLP studies, which tend to involve unnecessarily large numbers of animals [Tyl et al. (2002) used > 8,000 rats], and reliability appears to be accepted because of the numbers of animals that were used. Although using excessive numbers of animals is accepted as good science by the U.S. FDA, the use of arbitrarily large numbers of animals per group (> 20 animals per treatment group is common) actually violates guidelines in the NIH *Guide for the*